

# Stereoregular Precursors to Poly(*p*-phenylene) via Transition-Metal-Catalyzed Polymerization. 2. The Effects of Polymer Stereochemistry and Acid Catalysts on Precursor Aromatization: A Characterization Study

Douglas L. Gin,<sup>†</sup> Vincent P. Conticello,<sup>‡</sup> and Robert H. Grubbs\*

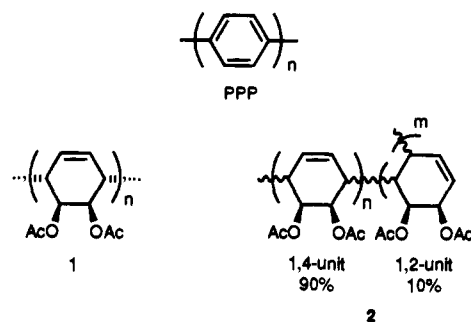
Contribution No. 8907 from the Arnold and Mabel Beckman Laboratories of Chemical Synthesis, California Institute of Technology, Pasadena, California 91125

Received December 27, 1993<sup>®</sup>

**Abstract:** The molecular weight and structural regularity of the polyphenylene produced from thermal conversion of two precursor polymers based on the acetyl derivative of 5,6-dihydroxy-1,3-cyclohexadiene depend on the stereochemistry of the precursor and the presence of aromatization catalysts. Two competing reactions occur during the bulk thermal conversion of these precursors: (1) thermal chain fracturing of the polymer and (2) thermally-induced acid elimination (aromatization) resulting in polyphenylene formation. The relative rates of these two processes ultimately determine the molecular weight of the final product and depend heavily upon the stereochemistry of the polymer backbone. For a 1,4-linked stereoregular precursor polymer made by nickel-catalyzed polymerization, the onset of chain degradation occurs before the onset of aromatization during heating. Consequently, this precursor only affords low-quality polyphenylene oligomers, despite having a regular stereochemistry that is ideal for facile *cis* pyrolytic acid elimination. On the other hand, the reverse relationships are true for its radically polymerized analog containing 10% 1,2-linkages. Although chain degradation still occurs during the pyrolysis of this atactic precursor, the relative amount of backbone fracturing is less than that of aromatization. The problems associated with the limited thermal stability of the precursor polymers can be overcome through the use of Brønsted and Lewis acid catalysts during bulk pyrolysis. Acids lower the onset temperature of aromatization to a regime well below that at which thermal chain scission can occur by selectively catalyzing the acid elimination reaction in both precursor polymers. However, characterization of the resulting polyphenylenes made from both polymers indicates that the structural regularity of the polyphenylene produced by the acid-catalyzed aromatization process depends entirely on the regiochemistry of the initial precursor. High molecular weight, structurally regular poly(*p*-phenylene) is produced only by the acid-catalyzed bulk aromatization of the 1,4-linked stereoregular polymer. Acid-catalyzed bulk pyrolysis of the radically polymerized analog only affords polyphenylene containing substantial amounts of 1,2-linkages.

## Introduction

We recently reported the design and synthesis of a highly 1,4-linked, stereoregular precursor polymer (**1**) to poly(*p*-phenylene) (PPP) via the transition-metal-catalyzed polymerization of functionalized 1,3-cyclohexadiene monomers.<sup>1,2</sup> Earlier attempts to design similar processible precursor routes to PPP using an intermediate polymer (**2**) made by radical polymerization<sup>3,4</sup> only afforded polyphenylene oligomers containing regiochemical defects.<sup>5</sup> The formation of low-quality polyphenylene oligomers was attributed to the random backbone stereochemistry and the 10% 1,2-linkages present in the radically



\* Author to whom correspondence should be addressed.

<sup>†</sup> Current address: Department of Chemistry, University of California, Berkeley, CA 94720.

<sup>‡</sup> Current address: Department of Polymer Science and Engineering, University of Massachusetts, Amherst, MA 01003.

<sup>®</sup> Abstract published in *Advance ACS Abstracts*, October 15, 1994.

(1) Gin, D. L.; Conticello, V. P.; Grubbs, R. H. *J. Am. Chem. Soc.*, preceding article in this issue. For brief overviews of this work, see: (a) Gin, D. L.; Conticello, V. P.; Grubbs, R. H. *J. Am. Chem. Soc.* **1992**, *114* (8), 3167. (b) Gin, D. L.; Conticello, V. P.; Grubbs, R. H. *Polym. Mater. Sci. Eng.* **1992**, *67*, 87.

(2) Polymer **1** is believed to be either a highly isotactic or a highly syndiotactic polymer with the repeat unit depicted in Figure 1. See ref 1 for the assignment and spectroscopic verification of the structure of **1**.

(3) (a) Ballard, D. G. H.; Courtis, A.; Shirley, I. M.; Taylor, S. C. *J. Chem. Soc., Chem. Commun.* **1983**, 954. (b) Ballard, D. G. H.; Courtis, A.; Shirley, I. M.; Taylor, S. C. *Macromolecules* **1988**, *21*, 294.

(4) McKean, D. R.; Stille, J. K. *Macromolecules* **1987**, *20*, 1787.

polymerized precursor.<sup>3,5</sup> By tailoring the stereochemistry and regiochemistry of the precursor polymer to facilitate thermal aromatization, we believed that polymer **1** would yield 100% para polyphenylene without significant chain degradation.<sup>1</sup>

The conversion of precursor polymers **1** and **2** to polyphenylene involves the thermally-induced elimination of acetic acid (eq 1). This type of elimination reaction is believed to proceed via a *cis* six-membered ring transition state.<sup>3b</sup> Thus, the *cis*-1,4-stereoregular structure of **1**<sup>2</sup> should be better suited for the facile formation of high-quality PPP (Figure 1) than the irregular structure of polymer **2**. We have discovered, however, that

(5) Internal report from ICI Chemicals and Polymers Ltd., Runcorn, U.K., based on neutron-scattering analysis of ICI polyphenylene performed at Durham University.

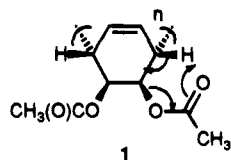
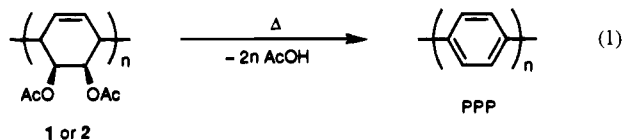


**Figure 1.** Optimum repeat unit stereochemistry for the cis elimination of acetic acid.



thermal conversion of these two precursor polymers to polyphenylene is not a straightforward process. Studies of the bulk pyrolysis of **1** and **2** suggest that actually two competing reactions occur during pyrolysis: (1) thermally-induced acid elimination leading to polyphenylene formation and (2) thermal chain degradation leading to a reduction in polymer molecular weight. Although the relative rates of these two competing reactions were found to depend heavily on the stereochemistry of the precursors, they were also found to be affected by the presence of acid catalysts. This paper describes the effect of precursor structure and acid catalysts on the rates of the two competing thermal reactions and on the quality of the resulting polyphenylene.

## Results and Discussion

**(A) Initial Thin Film Pyrolysis Studies.** In order to demonstrate that stereoregular precursor **1** could be easily converted to PPP, initial pyrolysis experiments were conducted on thin films of the material for subsequent spectroscopic analysis. Thin films of **1** were coated onto NaCl crystals from THF solution, aromatized by heating under argon at 310–340 °C, and then analyzed by IR spectroscopy.

IR spectroscopy is generally used to determine the structure and molecular weight of PPP samples.<sup>6–10</sup> Typically, the regiochemistry and the molecular weight of polyphenylene chains can be *qualitatively* determined by comparing the relative intensities of two sets of bands in the IR spectrum of the material: (1) a band at approximately 800–810 cm<sup>-1</sup>, which is due to the C–H out-of-plane bending of the 1,4-substituted benzene repeat units, and (2) two bands at approximately 760 and 697 cm<sup>-1</sup>, which are due to the C–H out-of-plane bending modes of the monosubstituted benzene end group units of the polymer (Figure 2).<sup>6–10</sup> For high molecular weight, completely 1,4-linked polyphenylene, the intensity of the 810 cm<sup>-1</sup> band is expected to be much greater than that of the two end group bands. In addition, the position of the repeat unit IR band generally shifts toward 800 cm<sup>-1</sup> in an asymptotic fashion as the number of consecutive 1,4-linked phenylene units increases. These two trends can be seen in the IR spectra of commercial *p*-oligophenyls of increasing molecular weight.

IR analysis of polyphenylene films made by pyrolysis of thin films of **1** cast on NaCl crystals was consistent with high

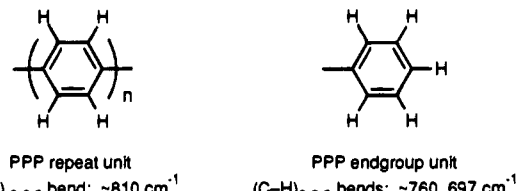


**Figure 2.** Repeat and end group units of PPP: characteristic IR bands.

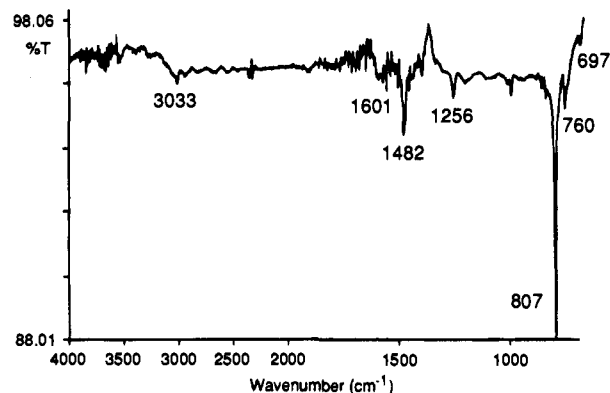


**Figure 3.** IR spectrum of a thin PPP film obtained by the pyrolysis of a thin film of **1** cast on NaCl.

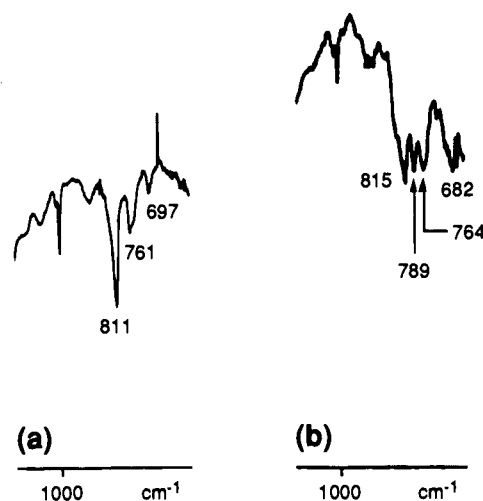


**Figure 4.** Partial IR spectra of polyphenylene films made by the pyrolysis of thin films of **2** cast on NaCl crystals, showing (a) PPP oligomers and (b) polyphenylene oligomers containing a substantial fraction of 1,2-units.

molecular weight PPP. As can be seen in Figure 3, a typical IR spectrum of a transparent, pale yellow-brown film obtained from pyrolysis of **1** on NaCl is dominated by an intense band at 807 cm<sup>-1</sup>, which is characteristic of PPP repeat units. The intensity of this repeat unit band is much stronger than that of the two end group bands at 760 and 696 cm<sup>-1</sup>. This high ratio of repeat unit to end group band intensities is a qualitative indication that the polyphenylene film made from **1** consists of high molecular weight, para-linked polyphenylene chains.<sup>6–10</sup> A band at 1745 cm<sup>-1</sup> characteristic of the C=O stretching of residual acetate groups is absent in Figure 3, indicating that aromatization of **1** is essentially complete. In contrast, IR analysis of thin polyphenylene films made from **2** under similar conditions gave inconsistent results. Occasionally, the IR spectra of the pyrolyzed films exhibit repeat unit and end group bands with relative intensities characteristic of 1,4-phenylene chains (Figure 4a). At other times, the IR spectra of the pyrolyzed thin films exhibit repeat unit and end group band intensities characteristic of PPP oligomers, plus an

(6) Kovacic, P.; Jones, M. B. *Chem. Rev.* **1987**, *87*, 357 and references therein.

(7) Elsenbaumer, R. I.; Shacklette, L. W. In *Handbook of Conducting Polymers*; Skotheim, T. A., Ed.; Marcel Dekker: New York, 1986; Vol. 1, Chapter 7 and references therein.

(8) Speight, J. G.; Kovacic, P.; Koch, F. W. *J. Macromol. Sci., Rev. Macromol. Chem.* **1971**, *C5* (2), 295 and references therein.

(9) Noren, G. K.; Stille, J. K. *Macromol. Rev.* **1971**, *5*, 385 and references therein.

(10) Chaturvedi, V.; Susumu, T.; Kaeriyama, K. *Macromolecules* **1993**, *26*, 2607.

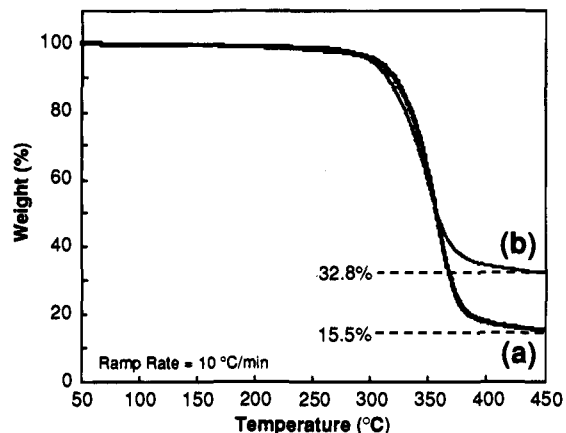


**Figure 5.** TGA profiles of (a) stereoregular polymer 1 and (b) radically polymerized polymer 2 under Ar flush.

additional band at  $789\text{ cm}^{-1}$  attributable to the C–H bending of 1,2-phenylene units (Figure 4b).<sup>11</sup> These results indicate that, at least as thin films on NaCl, stereoregular 1 consistently affords high-quality PPP whereas its atactic analog 2 generally affords low molecular weight material containing substantial amounts of 1,2-linked phenylene units.

**(B) Thermogravimetric Analysis of Bulk 1 and 2.** However, dramatically different results were obtained when the bulk pyrolysis of 1 and 2 was monitored and compared using thermogravimetric analysis (TGA). TGA monitors the weight loss of a material as a function of increasing temperature. Ideally, both 1 and 2 should lose 61.2% of their original weight if complete conversion to polyphenylene occurs during the heating process. However, TGA of pressed powder pellets or free-flowing powders of stereoregular 1 revealed that the polymer typically loses between 76 and 89% of its weight during bulk pyrolysis (Figure 5a). In addition, IR analysis of the TGA product of 1 revealed that only polyphenylene oligomers are produced. An IR band at approximately  $1745\text{ cm}^{-1}$  due to residual acetate carbonyl groups is also often observed in the bulk pyrolysis product of 1, indicating that acid elimination is incomplete despite the excessive weight loss. In contrast, radically polymerized 2 loses only slightly more weight than expected for complete aromatization when analyzed by TGA (Figure 5b). IR analysis of the TGA residue from 2 confirmed that only polyphenylene oligomers are formed. These TGA and IR results suggest that other reactions besides aromatization (i.e., acetic acid elimination) must be occurring during the bulk pyrolysis of 1 and 2.

Additional TGA and IR experiments indicated that small amounts of added NaCl (10 wt %) do not reduce the excessive mass loss observed during bulk pyrolysis of 1 or 2, nor does it improve the quality of the final products. Consequently, the presence of NaCl alone does not appear to be responsible for the discrepancies observed between bulk and thin film pyrolysis for these two polymers.

**(C) Effect of Polymer Structure on the Bulk Pyrolysis Process.** In order to elucidate the nature of the differences observed for 1 and 2 during TGA, the bulk pyrolysis of the two precursor polymers was examined by thermogravimetric analysis–mass spectrometry (TGA–MS). TGA–MS profiles monitoring the evolution of acetic acid, benzene, and phenol for 1 and 2 under inert atmosphere are presented in Figures 6 and 7, respectively.<sup>12</sup> The TGA trace of 1 indicates that this

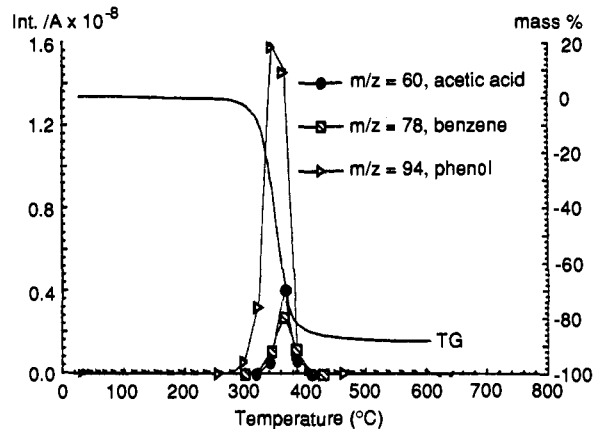


**Figure 6.** TGA–MS profile monitoring the evolution of acetic acid, benzene, and phenol for bulk pristine 1.

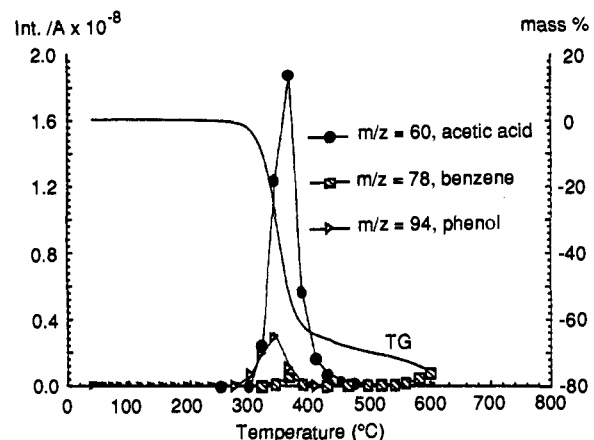


**Figure 7.** TGA–MS profile monitoring the evolution of acetic acid, benzene, and phenol for bulk pristine 2.

stereoregular polymer loses approximately 89% of its weight upon heating to 500 °C. The accompanying partial MS profile<sup>13</sup> indicates that benzene and phenol are generated to a much greater extent during pyrolysis than the desired elimination product, acetic acid (Figure 6). In contrast, the TGA–MS profile of 2 (Figure 7) shows that this radically polymerized polymer only loses approximately 65% of its original mass upon heating to 500 °C. In addition, acetic acid is generated to a much greater extent than benzene and phenol combined. Substantial amounts of benzene and phenol are still formed during the pyrolysis of 2; however, the proportion of these aromatic side-products compared to acetic acid is significantly smaller than in the case of 1.

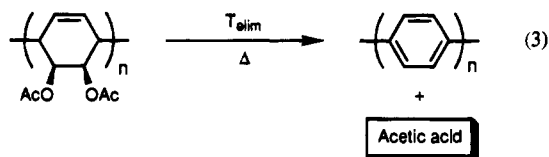
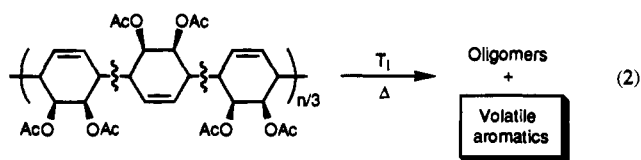
From these TGA–MS results, two things can be inferred. First, the pyrolysis of the two precursor polymers does not involve just a single process. There appears to be two competing reactions occurring during pyrolysis: (1) thermal degradation resulting in backbone fracturing and the evolution of small aromatic molecules (eq 2) and (2) thermally-induced acid elimination resulting in polyphenylene formation and the

(13) Mass spectrometry was used to monitor the evolution of TGA products with  $m/z$  ratios in the 1–150 range. However, only selected, abundant compounds indicative of aromatization or chain fracturing are displayed in the TGA–MS figures for the sake of simplicity (i.e., acetic acid, benzene, and phenol). Other abundant elimination products observed during the TGA–MS of pristine 1 and 2 are  $\text{CH}_2$  ( $m/z = 14$ ),  $\text{CH}_3$  ( $m/z = 15$ ),  $\text{CH}_4$  ( $m/z = 16$ ), and  $\text{CO}_2$  ( $m/z = 44$ ). Evolution of these compounds coincides with the elimination of acetic acid, and they are most likely fragmentation products of acetate groups or acetic acid via another mechanism. Extremely low levels of two unidentified compounds with  $m/z$  ratios of 51 and 56 were also detected during the thermal degradation of 1 and 2. Please see the supplementary material.

(11) Gordon, A. J.; Ford, R. A. *The Chemist's Companion*; John Wiley and Sons: New York, 1972; p 189.

(12) TGA–MS analysis was performed by Dr. George Wilkinson at ICI Chemicals and Polymers Ltd., Runcorn, U.K.

evolution of acetic acid (eq 3). Second, the onset temperatures



(and thus the relative rates) of these two competing reactions are highly dependent upon the structure of the polymers. The onset temperature for chain fracturing is hereby designated as  $T_f$ , and the onset temperature for acid elimination is designated as  $T_{elim}$ . In many respects,  $T_f$  is very similar to the ceiling temperature observed for some polyolefins.<sup>14</sup> For the 1,4-linked stereoregular polymer **1**,  $T_f$  is apparently lower than  $T_{elim}$ . In other words, the rate of chain degradation is apparently much greater than the rate of acid elimination during pyrolysis. Thus, as **1** is heated to higher temperatures, it undergoes a greater degree of backbone fracturing compared to polyphenylene formation. In contrast, its atactic analog **2** is apparently more thermally stable such that its  $T_f$  is slightly higher than  $T_{elim}$ . The degree of thermal chain fracturing is less than that of acetic acid elimination, and aromatization is the dominant reaction as **2** is heated to higher temperatures. However, a significant degree of backbone fracturing still occurs, as indicated by the presence of substantial levels of benzene and phenol in the TGA-MS profile of **2**.

We believe that the observed differences in the thermal chemistry of **1** and **2** arise primarily from the dramatic difference in backbone stereochemistry between the two precursor polymers. Although we have managed to design and synthesize a highly 1,4-linked, stereoregular precursor with the optimum stereochemistry for cis elimination,<sup>2b</sup> the stereoregular backbone has an inherent lower thermal stability that results in extensive chain scission before substantial conversion to PPP can occur. Although differences in polymer molecular weight and end groups<sup>15</sup> are also known to account for differences in thermal stability between polymers having similar substituents, we feel that these factors are only minor contributors in this case. The molecular weights of **1** and **2** are comparable and of roughly the same order of magnitude. The absolute molecular weights of **1** and **2** as determined by Viscotek GPC and low-angle laser light scattering (LALLS) analyses are presented in Table 1. Different polymer end groups may have an effect on the thermal

(14) This onset temperature for backbone fracturing ( $T_f$ ) is very similar to the ceiling temperature ( $T_c$ ) observed for many radically polymerized polyolefins.  $T_c$  is the temperature at which the opposing rates of polymerization and thermal depolymerization are equal, and the monomer is in equilibrium with the polymer. (See: Odian, G. *Principles of Polymerization*, 2nd ed.; Wiley-Interscience: New York, 1981; pp 268–271.) In the cases of **1** and **2**, however, use of the term  $T_c$  to describe the thermal degradation is technically incorrect. At the temperatures employed for pyrolysis, any monomer regenerated by thermal depolymerization or fracturing is immediately decomposed to the more stable aromatic along, as observed by mass spectrometry. Consequently, once thermal chain scission begins, it is a one-way process and a monomer-polymer equilibrium does not exist.

(15) (a) Shalaby, A. W. In *Thermal Characterization of Polymers*; Turi, E. A., Ed.; Academic Press: New York, 1981; Chapter 3. (b) Grassie, N.; Scott, G. *Polymer Degradation and Stabilisation*; Cambridge University Press: Cambridge, 1985; Chapter 2.

**Table 1.** Comparison of Viscotek GPC and LALLS Absolute Molecular Weight Data for Polymers **1** and **2**

polymer	Viscotek GPC analysis			LALLS analysis
	$M_n$	$M_w$	PDI	$M_w$
<b>1</b>	$2.68 \times 10^4$	$4.17 \times 10^4$	1.56	$4.94 \times 10^4$
<b>2</b>	$3.57 \times 10^4$	$9.32 \times 10^4$	2.61	$1.10 \times 10^5$

stability and the rate of thermal chain fracturing of **1** and **2**; however, their contribution to the thermal stability of the polymers in this case is uncertain. We were unable to directly detect or identify any end groups on **1** or **2** using  $^1\text{H}$  and  $^{13}\text{C}$  NMR spectroscopy.<sup>1,16,17</sup> In addition, the effect of polymer end groups on thermal stability varies from polymer system to polymer system, depending on both the nature of the end group and the structure and composition of the backbone.<sup>15</sup> Since we were unable to experimentally identify the end groups on **1** and **2**, we have attributed the observed differences in thermal degradation chemistry to the most obvious and most definitive difference in structure between the two polymers—backbone stereochemistry.

It should also be noted that elemental analysis of samples of **1** revealed that the amount of residual Ni in these samples is essentially negligible ( $\% \text{Ni} < 0.0041\%$ ).<sup>18</sup> Thus, the lower backbone thermal stability of **1** cannot be attributed to traces of Ni contaminant from its multistep synthesis.<sup>1</sup>

**(C) Effect of Acids on the Bulk Pyrolysis of 1 and 2.** In order to produce high-quality bulk PPP from precursor **1**, the acid elimination reaction (eq 2) was selectively accelerated by the use of catalysts, thereby lowering  $T_{elim}$  below  $T_f$ . Both Lewis acids such as  $\text{ZnCl}_2$ <sup>19</sup> and Brønsted acids such as 3,4-dichlorobenzenesulfonic acid (DCBSA) were found to catalyze the acid elimination reaction.  $\text{ZnCl}_2$  was a trace contaminant in early batches of **1** made using the  $\text{ZnCl}_2$ /acetyl chloride process.<sup>20</sup> These samples, containing approximately 1.6 wt% residual  $\text{ZnCl}_2$ , exhibited TGA weight losses consistent with complete conversion to polyphenylene. The effect of small quantities of  $\text{ZnCl}_2$  on the TGA-MS profile of polymer **1** is quite pronounced. For example, the addition of 2 wt%  $\text{ZnCl}_2$  to a sample of **1** made by a Zn-free route<sup>1</sup> has a dramatic effect

(16) Polymer **2** is synthesized by a traditional bulk radical polymerization process using an azobis(isobutyronitrile) initiator. Hence, the possible end groups for **2** are (1) the isobutyronitrile moiety (via initiation and the first addition step) and (2) the cyclohexenyl and 1,3-cyclohexadienyl groups (via conventional disproportionation, leading to chain transfer to monomer or polymer, or termination).

(17) Although the mechanism of bis[( $\eta^3$ -allyl)(trifluoroacetato)nickel(II)]-catalyzed polymerization of functionalized 1,3-cyclohexadienes has not been examined in detail, mechanistic studies of the catalyst with 1,3-butadiene suggest a syn-coordinative insertion process with 1,4-regioselectivity. Thus, one possible end group for polymer **1** is the  $\eta^1$ -allyl moiety (via the first insertion step). See: (a) Warin, R.; Teyssié, P.; Bourdaudurq, P.; Dawans, F. *J. Polym. Sci. Polym. Lett. Ed.* **1973**, *11* (3), 177. (b) Porri, L.; Aglietto, M. *Makromol. Chem.* **1976**, *177*, 1465. Other possible end groups may include the 1,3-cyclohexadienyl group, if hydride transfer (through  $\beta$ -elimination) is the dominant chain-transfer process, and the cyclohexenyl group, if the resulting Ni-H species from hydride elimination is able to reinsert into polymerization of additional monomer or inactive 1,3-cyclohexadienyl chain ends. See: Hadjiandreou, P.; Julémont, M.; Teyssié, P. *Macromolecules* **1984**, *17* (11), 2455. Although these chain-transfer processes have been postulated in bis[( $\eta^3$ -allyl)(trifluoroacetato)nickel(II)]-catalyzed butadiene polymerization, they have not been confirmed experimentally. Also, they may not necessarily be valid for the polymerization of functionalized 1,3-cyclohexadienes.

(18) Elemental Ni analysis on **1** was performed at Galbraith Laboratories Inc., Knoxville, TN.

(19) Other zinc halides (e.g.,  $\text{ZnBr}_2$  and  $\text{ZnI}_2$ ) exhibit a similar catalytic effect during bulk pyrolysis.

(20) The preparation of **1** by treatment of the corresponding trimethylsilyl ether derivative with acetyl chloride and  $\text{ZnCl}_2$  in diethyl ether is described in previous publications. See ref 1.

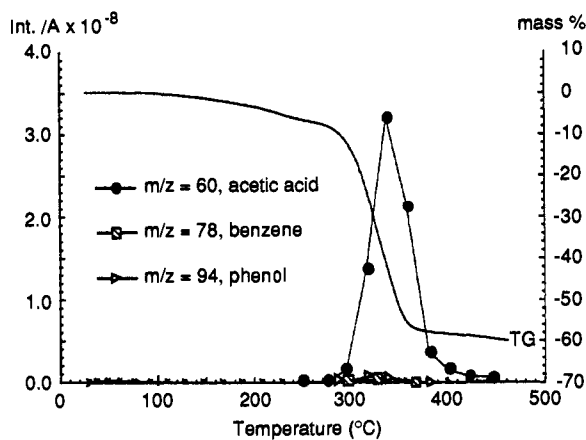


**Figure 8.** TGA-MS profile monitoring the evolution of acetic acid, benzene, and phenol for bulk 1 containing 2 wt %  $\text{ZnCl}_2$ .

on both the weight loss and the composition of the volatile compounds evolved during pyrolysis, as monitored by TGA-MS (Figure 8).<sup>12</sup> Instead of losing 89% of its weight upon pyrolysis, as in the case of the pristine material, **1** containing 2 wt %  $\text{ZnCl}_2$  only loses approximately 60% of its original weight (cf. Figures 6 and 8). This weight loss is close the value expected for complete conversion to polyphenylene (accounting for the residual  $\text{ZnCl}_2$  in the mixture). In addition, the MS profile showing the evolution of acetic acid, benzene, and phenol clearly indicates that the major elimination product is acetic acid. Thus, aromatization is the dominant thermal reaction in the presence of  $\text{ZnCl}_2$ .<sup>21</sup> Only extremely small (but non-zero) amounts of benzene and phenol are detected during pyrolysis when  $\text{ZnCl}_2$  is present. Apparently,  $\text{ZnCl}_2$  selectively accelerates the acid elimination (aromatization) reaction and lowers its onset temperature below that for thermal chain fracturing. This temperature reduction effect is small when only 2 wt %  $\text{ZnCl}_2$  is added to the polymer (cf. Figures 6 and 8); however, it becomes more pronounced with increasing amounts of added  $\text{ZnCl}_2$ . For example, the addition of 20 wt %  $\text{ZnCl}_2$  to the polymer lowers the onset of acetic acid elimination to approximately 200 °C (see the supplementary material).

When organic Brønsted acids were added to stereoregular precursor **1**, a similar catalytic effect was also observed. As can be seen from the TGA profile presented in Figure 9, the addition of 5 wt % DCBSA to **1** lowers the  $T_{\text{elim}}$  of the polymer from approximately 330 °C (where a combination of depolymerization and acid elimination simultaneously occurs in the pristine material) to approximately 180 °C. This temperature regime is well below the onset temperature for chain fracturing in the pristine polymer. The observed 60.7% weight loss is very close to the value expected for complete conversion of **1** to PPP, assuming that all of the DCBSA catalyst is also boiled away or decomposed during the process. The MS profile monitoring the evolution of acetic acid, benzene, and phenol during the TGA of **1** containing DCBSA (Figure 10)<sup>22</sup> clearly shows that acetic acid is the most abundant product generated

(21) Other abundant elimination products observed during the TGA-MS of **1** containing 10 wt %  $\text{ZnCl}_2$  and 5 wt % DCBSA are  $\text{CH}_2$ ,  $\text{CH}_3$ ,  $\text{CH}_4$ , and  $\text{CO}_2$ . Evolution of these compounds coincides with the elimination of acetic acid, and they are most likely fragmentation products of acetate groups or acetic acid via another mechanism. During the TGA-MS study of **1** containing 5 wt % DCBSA,  $\text{SO}$  ( $m/z = 48$ ) and  $\text{SO}_2$  ( $m/z = 64$ ) were detected in addition to the four compounds mentioned above. The  $\text{SO}$  and  $\text{SO}_2$  (and low levels of accompanying benzene) undoubtedly come from the thermal decomposition of the DCBSA at ca. 200 °C. Extremely low levels of two unidentified compounds with  $m/z$  ratios of 51 and 56 were also detected during the thermal degradation of **1** containing both acid catalysts. Please refer to the supplementary material for these additional MS profiles.

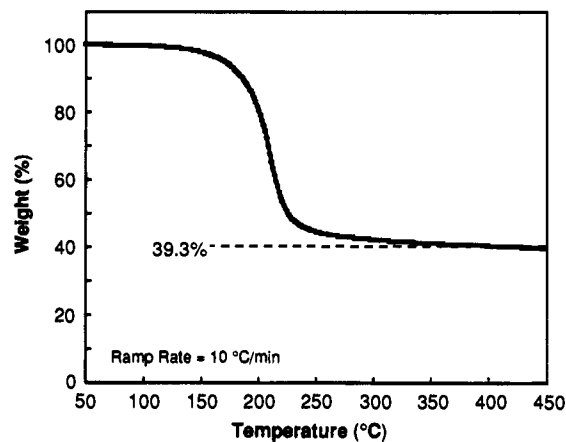


**Figure 9.** TGA profile (under Ar flush) of bulk 1 containing 5 wt % DCBSA.

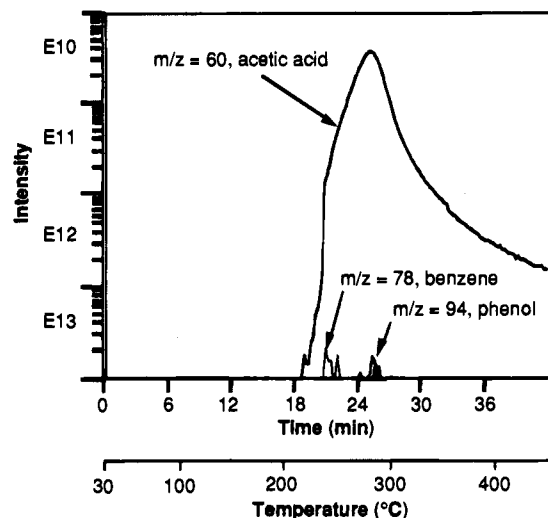


**Figure 10.** MS profile showing the evolution of acetic acid, benzene, and phenol during the TGA of bulk 1 containing 5 wt % DCBSA. (Note that the vertical axis is a logarithmic scale).

of the three.<sup>21</sup> In fact, the levels of benzene and phenol generated are more than 3 orders of magnitude lower than that of acetic acid. Thus, thermal chain fracturing does not occur to any significant extent in the presence of the Brønsted acid. Unlike  $\text{ZnCl}_2$ , the addition of more DCBSA to **1** does not significantly lower the  $T_{\text{elim}}$  of the polymer much below 170 °C. There are, however, two distinct two advantages in using organic Brønsted acids such as DCBSA over inorganic Lewis acids such as  $\text{ZnCl}_2$ : (1) The catalytic effect is more pronounced with the organic acids than  $\text{ZnCl}_2$  on both a per weight and a per mole basis (cf. Figures 8 and 9).<sup>23</sup> (2) The organic acids can be easily removed from the final product by simply heating the as-synthesized polyphenylene to higher temperatures.<sup>24</sup> The major drawback in using the zinc halides as aromatization catalysts is that these compounds are difficult, if not impossible, to remove from the insoluble polyphenylene matrix even by repeated washing with water or THF.<sup>25</sup>

It should be noted that acids have also been also found to

(22) Additional TGA-MS analyses were performed by Dr. Andrew R. McGhie at the Laboratory for Research on the Structure of Matter at the University of Pennsylvania, Philadelphia, PA.

(23) The greater temperature reduction effect observed for DCBSA is probably due to the fact that DCBSA (dihydrate) melts at 71–72 °C—and is thus better able to diffuse through the precursor polymer matrix at a lower temperature—whereas  $\text{ZnCl}_2$  does not melt until 283 °C. See: *CRC Handbook of Chemistry and Physics*, 65th ed.; Weast, R. C., Astle, M. J., Beyer, W. H., Eds.; Chemical Rubber Co.: Baton Rouge, LA, 1985; pp C-122, B-159.

catalyze the aromatization of polymer **2**. Using TGA, Wilson et al.<sup>26</sup> and Ober et al.<sup>27</sup> found that catalytic amounts of organic Brønsted acids lowered the aromatization temperature of **2**. However, they were not able to directly verify that acid elimination was the reaction being catalyzed by the protic acids. Using TGA-MS, we have been able to directly determine that acetic acid elimination is the dominant thermal reaction when **2** is pyrolyzed in the presence of 10 wt % ZnCl<sub>2</sub> or 5 wt % DCBSA. During TGA, the MS profiles monitoring the evolution of acetic acid, benzene, and phenol clearly show that acetic acid is the major elimination product when the two acid catalysts are added to **2**. The levels of benzene and phenol generated are at least 1.5–2 orders of magnitude lower than that of acetic acid when the acid-catalyzed samples are heated from 150 to 450 °C. (In the case of the DCBSA catalyst, low levels of benzene are also generated at approximately 200 °C from the thermal decomposition of the DCBSA catalyst.) Significant levels of benzene are not observed until approximately 500 °C, at which point thermal degradation of the polyphenylene occurs (see the supplementary material).

Lewis and Brønsted acids also catalyze the aromatization of some of the other derivatives of polymers **1** and **2**,<sup>28,29</sup> mentioned in our previous publications. Thus, acid-catalyzed thermal aromatization appears to be a general phenomenon for polymers based on the acyl derivatives of 5,6-dihydroxy-1,3-cyclohexadiene.<sup>29</sup> However, the acid-catalyzed aromatization of the acetoxy polymers **1** and **2** provides the most efficient route to polyphenylene in terms of overall mass loss upon conversion<sup>29</sup> and in terms of the quality of the final product.<sup>28</sup>

**(D) Polyphenylene Characterization: The Combined Effect of Precursor Stereochemistry and Acid Catalysts on the Quality of the Polyphenylene Formed.** Although acid-

(24) Elemental analysis of PPP samples made from **1** using 5 wt % DCBSA indicated that these samples contain only trace amounts of residual sulfur (less than 0.5 wt %) after heating to a maximum temperature of 400 °C under Ar during pyrolysis. Anal. Calcd for (C<sub>6</sub>H<sub>4</sub>)<sub>n</sub>: C, 94.70; H, 5.30. Found: C, 91.52; H, 5.06; N, 0.11; S, 0.43. For a PPP sample made using 5 wt % DCBSA but heated to a maximum temperature of 450 °C under Ar, the sample had the following composition. Found: C, 92.28; H, 5.07; N, 0.03; S, 0.52. TGA of pure DCBSA revealed that the acid is completely decomposed or boiled away at temperatures greater than 300 °C. ZnCl<sub>2</sub> cannot be removed from the polyphenylene samples in a similar manner since it boils at 732 °C, above the decomposition temperature of PPP itself. See: *CRC Handbook of Chemistry and Physics*, 65th ed.; Weast, R. C., Astle, M. J., Beyer, W. H., Eds.; Chemical Rubber Co.: Baton Rouge, LA, 1985; p B-159.

(25) Elemental analysis of thoroughly washed polyphenylene samples made using 10 wt % ZnCl<sub>2</sub> as an aromatization catalyst indicated that these samples contain a large percentage of material which is neither carbon nor hydrogen and is assumed to be ZnCl<sub>2</sub>. Zinc analysis could not be performed on the samples due to their insolubility.

(26) Wilson, D. R.; Jathavedam, H.; Thomas, N. W. *Contemporary Topics in Polymer Science*; Salome, J. C., Riffle, J. S., Eds.; Plenum: New York, 1991; Vol. 7.

(27) Kim, H. K.; Ober, C. K. *Polym. Bull.* **1992**, *28*, 33.

(28) DCBSA and ZnCl<sub>2</sub> were also tested on the other functionalized derivatives of polymers **1** and **2** mentioned in the preceding article (ref 1). Either they have no beneficial effect on the pyrolysis process, or they only produce low-quality polyphenylene oligomers. For example, DCBSA and ZnCl<sub>2</sub> have no effect on the pyrolysis of the methoxycarbonyl derivative of **2** made by the ICI process. The aromatization of this derivative is base-catalyzed (see refs 3 and 26). ZnCl<sub>2</sub> has no effect on the bulk pyrolysis of the trimethylsilyl ether derivative of **1**, but strong Brønsted acids catalyze the hydrolysis of this polymer to the corresponding stereoregular hydroxy polymer in the presence of trace amounts of water. Both DCBSA and ZnCl<sub>2</sub> catalyze the thermal dehydration of the stereoregular hydroxy derivative of **1**, but IR and TGA analyses indicated that only PPP oligomers are formed by this process.

(29) Lewis and Brønsted acids were also found to generally catalyze the aromatization of other ester derivatives of **1** and **2**, such as the benzoate derivative of **1** described in the preceding article. However, in terms of percent mass loss upon conversion to polyphenylene, use of the acetoxy polymers **1** and **2** is still the most efficient route to polyphenylene. Acetic acid is the smallest acid that can be eliminated in the series of ester derivatives, thus offering the best weight yield upon aromatization.

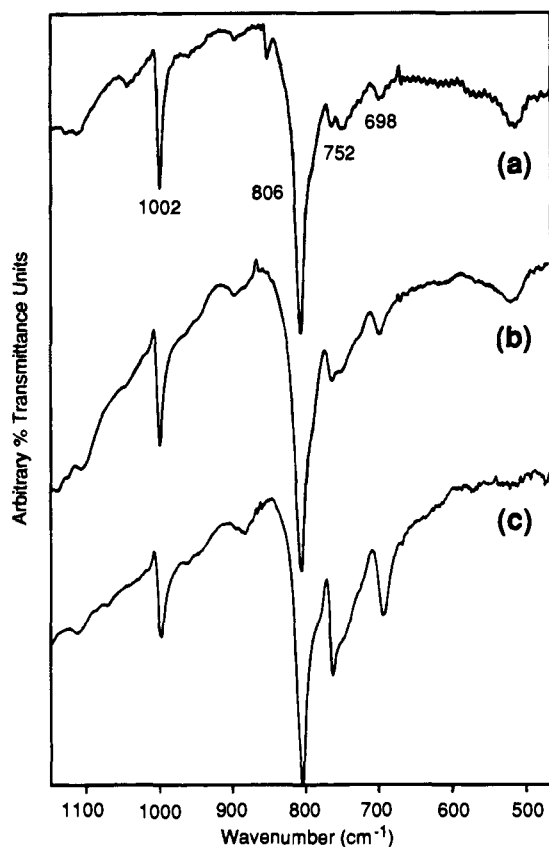


**Figure 11.** Partial IR spectra (KBr mull) of the polyphenylene samples made from the bulk pyrolysis of polymer **1** containing (a) 5 wt % DCBSA, (b) 10 wt % ZnCl<sub>2</sub>, and (c) no acid catalyst.

catalyzed aromatization appears to be a general phenomenon for **1** and **2**, the molecular structure and the spectroscopic properties of the resulting polyphenylenes were found to be drastically different. The quality of the resulting polyphenylene depends on *both* the regiochemical structure of the precursor polymer and the use of acid catalysts. The following characterization studies on the polyphenylenes obtained from the catalyzed and uncatalyzed bulk pyrolysis of **1** and **2** clearly demonstrate this dependence.

**(i) IR Analysis.** IR analysis of the bulk pyrolysis products of **1** and **2** revealed that high molecular weight, 1,4-linked PPP is formed *only* via the acid-catalyzed aromatization of the highly 1,4-linked precursor **1**. As can be seen from Figure 11a,b, the IR spectra of the bulk polyphenylene samples made from DCBSA- and ZnCl<sub>2</sub>-catalyzed aromatization of pressed pellets of **1** are dominated by an intense band at 806 cm<sup>-1</sup> due to PPP repeat units. The two end group IR bands at 760 and 696 cm<sup>-1</sup> are extremely weak in comparison. In addition, the absence of any other bands in the 600–840-cm<sup>-1</sup> region of the IR spectrum indicates that the amount of other types of aromatic units (e.g., cross-links<sup>30</sup> or other regioisomers) in these two materials is essentially negligible. These results are consistent with high molecular weight, structurally regular PPP. In sharp contrast, the IR spectra of the polyphenylene samples similarly prepared from **2** using the same acids exhibit repeat unit and end group bands with relative intensities characteristic of only very short

(30) DSC studies of **1** containing 5 wt % DCBSA and 10 wt % ZnCl<sub>2</sub> revealed that these mixtures exhibit a small exotherm at approximately 112–120 °C prior to the major aromatization exotherm beginning at 180–200 °C (see the Supplementary Material). The first exotherm is not observed in the DSC profile of pristine **1**. The fact that the 1/acid mixtures are still completely soluble in THF at ambient temperature, even after being heated past the first exotherm, suggests that the low-temperature exotherm is not due to acid-catalyzed cross-linking.

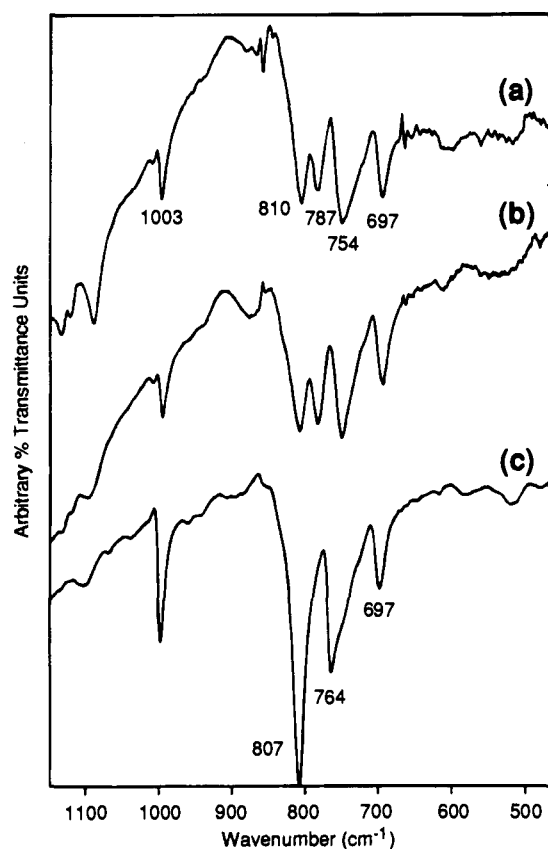


**Figure 12.** Partial IR spectra (KBr mull) of the polyphenylene samples made from the bulk pyrolysis of polymer **2** containing (a) 5 wt % DCBSA, (b) 10 wt %  $\text{ZnCl}_2$ , and (c) no acid catalyst.

runs of 1,4-linked phenylene units (Figures 12a,b). Furthermore, the IR spectra of these bulk polyphenylene samples both exhibit an additional IR band at  $789\text{ cm}^{-1}$ , characteristic of 1,2-linked phenylene units (just as in the case of pyrolysis of thin films of **2** on NaCl crystals).<sup>11,31</sup> The IR spectra of the bulk pyrolysis products of pristine **1** and **2** indicate that the aromatic products are only oligomeric in nature and do not contain any 1,2-units (Figures 11c and 12c). Judging by the relative intensities of the repeat unit and end group bands, the molecular weights of these PPP oligomers are only slightly higher than that of *p*-sexiphenyl.

The latter observations, coupled with the TGA-MS results, suggest that, in the absence of acid catalysts, chain scission in polymer **2** occurs predominantly at the 1,2-linkages to afford short, linear polyphenylene segments (i.e., the 1,2-defect sites are the thermal weak points in the polymer). In the presence of acid catalysts, chain scission does not occur to any significant extent during bulk pyrolysis. Hence, the 10% 1,2-units in polymer **2** become 1,2-phenylene units in the final material,

(31) The four-band IR spectra of the irregular polyphenylene made by the  $\text{ZnCl}_2$ - and DCBSA-catalyzed bulk pyrolyses of **2** (Figure 12) and the thin film pyrolysis of pristine **2** on NaCl (Figure 4b) are essentially the same. In addition, the IR spectra of the PPP made by the  $\text{ZnCl}_2$ - and DCBSA-catalyzed bulk pyrolyses (Figure 11) and thin film pyrolysis on NaCl of **1** (Figure 3) are also essentially identical. These observations suggest that, for thin films of the precursors cast onto NaCl crystals, the surface of the crystal may possibly be acting as a weak Lewis acid (i.e., the  $\text{Na}^+$  sites) and catalyzing the acid elimination reaction via coordination of the acetate carbonyl groups. This weak coordinative effect would be expected to depend largely on the ratio of the surface area of the NaCl to the mass of the precursor in contact with it. Unlike DCBSA and  $\text{ZnCl}_2$ , which melt at 72 and 283 °C, respectively, NaCl does not melt until 801 °C. Thus catalytic amounts of NaCl added to **1** and **2** would not be expected to have a significant effect on the bulk pyrolysis (as shown in section A) since the NaCl cannot melt and diffuse through the precursor matrix except at extremely high temperatures.

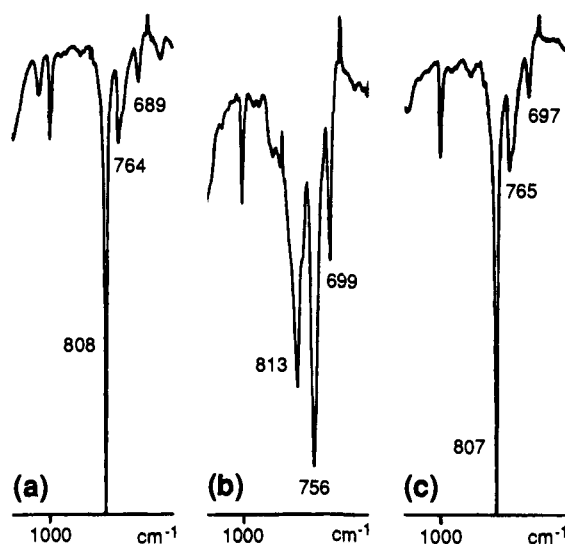


**Figure 13.** Partial IR spectra of polyphenylene films on NaCl crystals made from the pyrolysis of thin films of **2** containing (a) 5 wt % DCBSA, (b) 10 wt %  $\text{ZnCl}_2$ , and (c) no acid catalyst.

thereby generating irregular polyphenylene instead of completely linear material.

These observations suggest an interesting set of relationships among precursor structure, acid catalysts, and product structure: *acid catalysts are essential for suppressing the amount of chain fracturing during the pyrolysis of 1 and 2, but it is the regiochemical structure of the precursor polymer that ultimately determines the structural regularity of the polyphenylene formed.*

It is interesting to note that, in the earlier studies of Brønsted acid-catalyzed pyrolysis of **2**, Wilson et al. found that thin polyphenylene films formed by acid-catalyzed pyrolysis were not significantly different by IR analysis from material obtained by the pyrolysis of the pristine polymer.<sup>26</sup> However, our current IR studies indicate that the polyphenylene samples produced by the acid-catalyzed *bulk* pyrolysis of **2** are structurally very different from the samples made using the pristine polymer. These differences suggest that the effectiveness of the organic acid catalysts depends on the sample thickness. It is reasonable to assume that in thin film pyrolysis, where the surface area to mass ratio is very high, even relatively nonvolatile organic acids such as DCBSA sublime prior to the onset of catalyzed elimination. Thus, organic acids such as DCBSA appear to be ineffective during thin film pyrolysis. However, during bulk pyrolysis of pressed powder pellets where the surface area to mass ratio is much lower, the 5 wt % organic acid catalyst is effective because it is better confined in the sample matrix and less susceptible to premature sublimation prior to conversion. Unlike the more volatile organic acids,  $\text{ZnCl}_2$  is an effective catalyst even during thin film pyrolysis because of its extremely low vapor pressure and high boiling point (bp = 732 °C) which allow it to remain in the thin films throughout the entire thermal conversion process without subliming or decomposing. This working hypothesis is supported by the following observations: the IR spectra of thin polyphenylene films obtained from pristine **2** and **2** containing 5 wt % DCBSA were found to be virtually identical, whereas the IR spectrum of a thin polyphenylene film made from **2** with  $\text{ZnCl}_2$  has the same four bands in the 600–840- $\text{cm}^{-1}$  region as samples made from DCBSA- and  $\text{ZnCl}_2$ -catalyzed *bulk* pyrolysis (see Figure 13).

(ii) **Morphology.** The acid catalysts used to catalyze the aromatization of **1** and **2** have a dramatic effect on the morphology of the final products. When pressed pellets of **1** and **2** containing DCBSA or  $\text{ZnCl}_2$  are pyrolyzed, both the high-

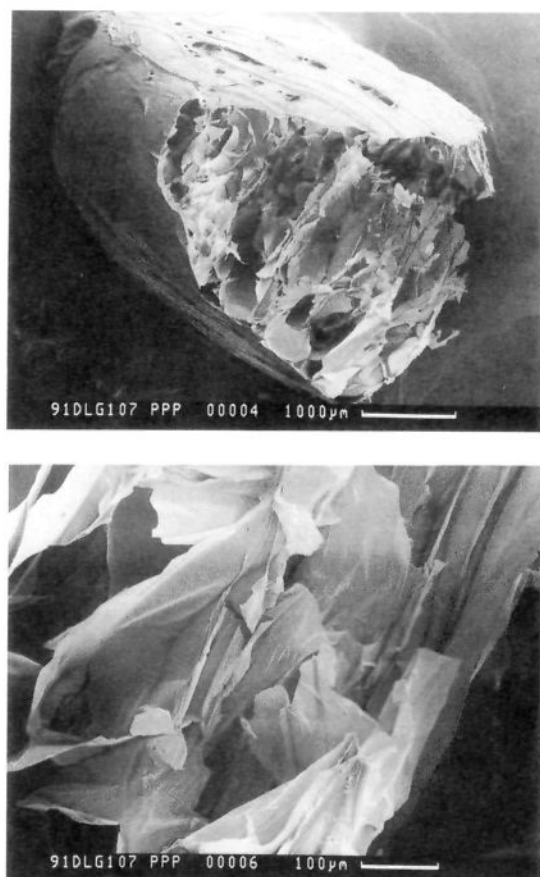


**Figure 14.** SEM photographs of the cross section of a "spongy" PPP foam made from the bulk pyrolysis of a pressed powder pellet of **1** containing 5 wt % DCBSA: (a)  $\times 20$  magnification; (b)  $\times 170$  magnification.

quality PPP made from **1** and the irregular polyphenylene made from **2** are formed as resilient black foams (Figures 14 and 15). All of these PPP and polyphenylene foams are amorphous by powder X-ray diffraction (PXRD) analysis. The foams have roughly the same shape as the original pressed pellets, but their dimensions are larger due to the interior void volume produced by the rapid elimination of acetic acid. Often, the interiors of these foams are filled with lustrous, flaky fibers (Figure 14). In contrast, when pressed pellets of pristine **1** or **2** are pyrolyzed, the resulting polyphenylene oligomers are obtained as brittle, orange-brown films that are semicrystalline by PXRD analysis. Apparently, without acid catalysts to accelerate the aromatization reaction, the pristine precursors flow and lose their original shape as they undergo a combination of acid elimination and chain fracturing.

To our knowledge, the high-quality PPP samples made by the acid-catalyzed bulk aromatization of **1** are the first examples of amorphous PPP.<sup>32</sup> "PPP" made by previous synthetic routes have been almost always semicrystalline.<sup>6-9</sup> Because of this difference in morphology, the molecular weight of the PPP samples made by the acid-catalyzed bulk aromatization of **1** may actually be substantially higher than that of previous "PPP" samples in the literature if compared by IR analysis. The intensities of the IR bands used for determining the relative amount of phenylene end groups actually shrink relative to the intensity of the repeat unit band when semicrystalline "PPP" samples are annealed to higher crystalline perfection.<sup>6,33</sup> Since a higher degree of crystallinity favors less intense end group IR bands, the chain lengths of our amorphous PPP samples may

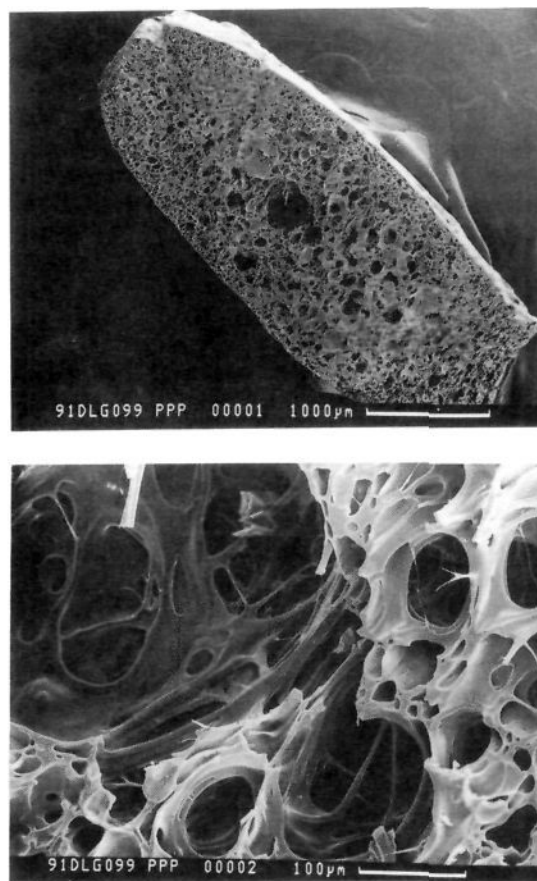


**Figure 15.** SEM photographs of the cross section of a brittle PPP foam made from the bulk pyrolysis of a pressed powder pellet of **2** containing 10 wt % ZnCl<sub>2</sub>: (a)  $\times 27$  magnification; (b)  $\times 230$  magnification.

actually be underestimated by IR analysis, compared to semicrystalline materials.

(iii) <sup>13</sup>C CPMAS Solid-State NMR Analysis. In order to verify the differences in molecular weight and regiochemistry observed by IR analysis, the bulk polyphenylene samples prepared from **1** and **2** were also characterized by <sup>13</sup>C cross-polarization magic angle spinning (CPMAS) NMR spectroscopy. Typically, <sup>13</sup>C solid-state NMR spectra of *p*-oligophenyls consist of two resonances at 128 and 139 ppm which are characteristic of the protonated and nonprotonated aromatic carbons, respectively (Figure 16).<sup>34-37</sup> The integral ratio of the protonated and nonprotonated aromatic carbons (*r*) decreases with the number

(32) The lack of crystallinity in the PPP samples made from **1** simply means that the rigid-rod polymer chains are not regularly aligned and positioned with respect to one another. The lack of crystallinity cannot be used to draw any direct conclusions about the molecular structure or the regioregularity of the polymer chains since PXRD is not a direct probe of these factors. IR spectroscopy, on the other hand, directly confirms that the amorphous PPP samples made by the acid-catalyzed bulk pyrolysis of **1** consist of structurally regular, high molecular weight PPP chains. The lack of crystallinity in these PPP samples can be rationalized in two ways: (1) The PPP is made from an amorphous, coiled precursor polymer; thus order is not an intrinsic property of the system. (2) From IR analysis, the molecular weight of the PPP made from acid-catalyzed pyrolysis of **1** is much higher than conventional oligomeric "PPP". Thus, it would be much more difficult to anneal these high molecular weight PPP chains into a crystalline array during thermal conversion, especially at the lower aromatization temperatures afforded by the acid catalysts.

(33) Yaniger, S. I.; Rose, D. J.; McKenna, W. P.; Eyring, E. M. *Macromolecules* **1984**, *17*, 2579.

(34) Murray, D. P.; Dechter, J. J.; Kispert, L. D. *J. Polym. Sci., Polym. Lett. Ed.* **1984**, *22*, 519.

(35) Barbarin, F.; Berthet, G.; Blanc, J. P.; Fabre, C.; Germain, J. P.; Hamdi, M.; Robert, H. *Synth. Met.* **1983**, *6*, 53.



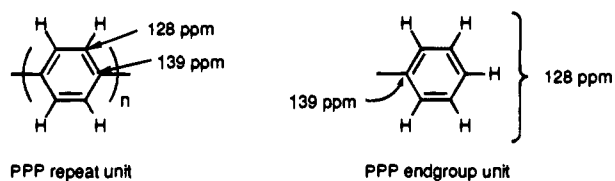


**Figure 16.** Repeat and end group units of PPP and *p*-oligophenyls: characteristic  $^{13}\text{C}$  CPMAS NMR signals.

**Table 2.** Ratio of Protonated to Nonprotonated Aromatic Carbons as a Function of the Number of Phenyl Rings for a Series of *p*-Oligophenyls<sup>a</sup>

compound	chain length ( $n$ )	ratio of protonated to nonprotonated carbons ( $r$ )
biphenyl	2	5.0
<i>p</i> -terphenyl	3	3.5
<i>p</i> -quaterphenyl	4	3.0
<i>p</i> -sexiphenyl	6	2.6

$$^a r = \frac{2n+1}{n-1} \quad (4)$$

of consecutive 1,4-linked phenyl rings in the chains ( $n$ ) according to eq 4 (see Table 2).<sup>34</sup> As the number of successive 1,4-phenylene units increases in the polyphenylene samples, the integral ratio  $r$  should asymptotically approach a minimum value of 2, the value for an infinitely long PPP chain. Consequently, the integral ratio  $r$  can be used to extrapolate the approximate average molecular weight of polyphenylene samples.

The  $^{13}\text{C}$  CPMAS NMR spectra of five of the six bulk polyphenylene samples are presented in Figure 17. The polyphenylene oligomers made by the bulk pyrolysis of pristine **1** were not analyzed by this technique because both TGA-MS and IR analyses verified that these samples are obviously oligomeric in nature. In addition, the large amount of chain fracturing that occurs during the bulk pyrolysis of pristine **1** made it difficult to synthesize enough oligomer to pack an NMR sample rotor (10–15% pyrolysis yield).

As can be seen in Figure 17, all five of the samples exhibit the two  $^{13}\text{C}$  resonances at 128 and 139 ppm characteristic of protonated and nonprotonated aromatic carbons.<sup>38</sup> In addition, there are no signals due to residual carbonyl groups in the 160–190-ppm region or due to saturated carbon centers in the 10–50-ppm range. Unfortunately, the relative molecular weights of the five bulk polyphenylene samples could not be accurately compared using  $^{13}\text{C}$  CPMAS NMR spectroscopy because of anomalies in the  $^{13}\text{C}$  integral ratios. The  $^{13}\text{C}$  integral ratios of the five polyphenylene samples are summarized in Table 3.<sup>39</sup> The two high-quality PPP samples made via the acid-catalyzed bulk aromatization of **1** exhibit anomalous integral ratios of nearly 1:1, a value well below the theoretical minimum expected

(36) Brown, C. E.; Khoury, I.; Bezoari, M. D.; Kovacic, P. *J. Polym. Sci., Polym. Chem. Ed.* **1982**, *20*, 1697.

(37) Brown, C. E.; Jones, M. B.; Kovacic, P. *J. Polym. Sci., Polym. Lett. Ed.* **1980**, *18*, 653.

(38) The signals in the  $^{13}\text{C}$  CPMAS NMR spectra of the four amorphous polyphenylene samples made via the DCBSA- and  $\text{ZnCl}_2$ -catalyzed pyrolyses of **1** and **2** are much broader than those of the semicrystalline PPP oligomers made from pyrolysis of pristine **2** (and that of crystalline *p*-oligophenyls). In fact, the resonances are so broad that it is impossible to resolve the aromatic carbons from different regiochemical linkages (i.e., 1,2- and 1,3-units). The differences in line width between the various bulk polyphenylene samples can be attributed to the fact that the original pulse parameters were selected using crystalline *p*-quaterphenyl and *p*-sexiphenyl as standards. Thus, these pulse parameters may not be optimal for amorphous samples. Spectra with better resolution and signal-to-noise were obtained for the two amorphous polyphenylene samples made from the DCBSA-catalyzed aromatizations of **1** and **2** using a shorter contact pulse of 1 ms. However, the integral ratios did not change significantly.

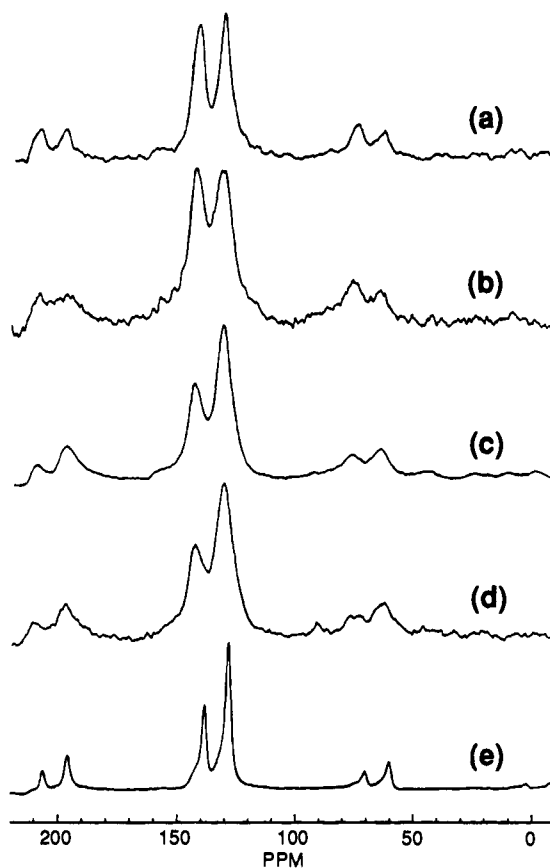


**Figure 17.**  $^{13}\text{C}$  CPMAS NMR spectra of the polyphenylene samples made from the bulk pyrolysis of (a) **1** containing 5 wt % DCBSA, (b) **1** containing 10 wt %  $\text{ZnCl}_2$ , (c) **2** containing 5 wt % DCBSA, (d) **2** containing 10 wt %  $\text{ZnCl}_2$ , and (e) pristine **2**.

**Table 3.** Integral Ratios of Protonated (128 ppm) and Nonprotonated (139 ppm) Carbons in the  $^{13}\text{C}$  CPMAS NMR Spectra in Figure 17

polyphenylene $^{13}\text{C}$ CPMAS spectrum	composition of precursor	integral ratio <sup>a</sup> ( $I_{128 \text{ ppm}}/I_{139 \text{ ppm}}$ )
Figure 17a	<b>1</b> + 5 wt% DCBSA	1.05
Figure 17b	<b>1</b> + 10 wt% $\text{ZnCl}_2$	1.22
Figure 17c	<b>2</b> + 5 wt% DCBSA	1.84
Figure 17d	<b>2</b> + 10 wt% $\text{ZnCl}_2$	1.75
Figure 17e	pristine <b>2</b>	1.91

<sup>a</sup> Integrals were obtained by the standard integration procedures on the NMR spectrometer. These values were checked by deconvoluting and curve-fitting selected spectra to obtain more accurate integral values.

for infinitely long PPP chains (see Figure 17a,b). Thus, extrapolation of molecular weights in these two cases using eq 4 is impossible.

Similar intensity anomalies have also been encountered by other researchers who have used  $^{13}\text{C}$  CPMAS NMR spectroscopy to characterize other "PPP" samples in the literature.<sup>36</sup> Such intensity anomalies have generally been attributed to instrumental problems.<sup>34</sup> Unfortunately, we were not able to identify any instrumental parameters that would affect the  $^{13}\text{C}$  integral ratios of the samples to this degree.<sup>38,39</sup> We also could not find any obvious correlation between these intensity

(39) Typically, recycle delays of at least five times  $^1\text{H}$   $T_1$  are required to ensure complete relaxation of the magnetization between scans. See: Sanders, J. K. M.; Hunter, B. K.; *Modern NMR Spectroscopy, A Guide for Chemists*; Oxford University: Oxford, U.K., 1987; p 43. Proton spin-lattice relaxation time ( $^1\text{H}$   $T_1$ ) experiments indicated that the two amorphous polyphenylene samples made from DCBSA-catalyzed pyrolyses of **1** and **2** have  $^1\text{H}$   $T_1$  values of 0.64 and 0.15 s, respectively. Hence, the 5-s pulse delay initially employed was more than enough to permit complete relaxation of the magnetization between pulses.

**Table 4.** Thermal Stabilities (under Ar) of the Polyphenylene Samples Made by the Catalyzed and Uncatalyzed Bulk Pyrolysis of Polymers **1** and **2**

polyphenylene preparation		polyphenylene thermal stability <sup>b</sup>	
precursor composition	pyrolysis conditions <sup>a</sup>	% wt loss at 500 °C	onset of decomp (°C)
<b>1</b> + 5 wt% DCBSA	A	3–5	545
<b>1</b> + 10 wt% ZnCl <sub>2</sub>	B	15	418
pristine <b>1</b>	A	6	487
<b>2</b> + 5 wt% DCBSA	A	5	526
<b>2</b> + 10 wt% ZnCl <sub>2</sub>	B	14	434
pristine <b>2</b>	A	4	549

<sup>a</sup> A: 100 °C (1 h) → (2 °C/min) → 300 °C (5 h) → (2 °C/min) → 400 °C (0.1 h). B: 100 °C (1 h) → (2 °C/min) → 340 °C (5 h). <sup>b</sup> TGA was performed with a ramp rate of 10 °C/min from 100 to 700 °C under Ar flush.

anomalies with sample-related factors such as morphology or unpaired spin density. Differences in morphology among the various samples (amorphous vs crystalline) may account for signal broadness in some of the polyphenylene samples in Figure 17;<sup>38</sup> however, there is no apparent correlation since four of the samples are amorphous but only two exhibit the anomalous integral ratios. Magnetic measurements were also performed to determine whether the anomalous <sup>13</sup>C intensity distributions might be due to differences in the samples' unpaired spin densities. "PPP" samples in the literature typically exhibit high spin densities in the undoped state,<sup>6</sup> and higher spin densities in samples have been found to have an effect on NMR relaxation parameters.<sup>34</sup> Unfortunately only the high-quality PPP made from **1** using DCBSA and the phenylene oligomers made from pristine **2** were found to exhibit significant unpaired spin densities on the order of 10<sup>19</sup> and 10<sup>20</sup> spins/g, respectively.<sup>40</sup> The spin densities of the other three polyphenylene samples analyzed by <sup>13</sup>C NMR were all found to be below the detection limit of the spectrometer (<10<sup>16</sup> spins/g). Again, there is no obvious relationship between the samples exhibiting anomalous <sup>13</sup>C integral ratios and their unpaired spin densities.

Hence, definitive conclusions regarding the relative molecular weights of the polyphenylene samples cannot be drawn from this preliminary solid-state <sup>13</sup>C NMR study because of the anomalous intensity distributions observed for the PPP samples made from **1**. From <sup>13</sup>C chemical shift assignments, it is quite obvious that all of the polyphenylene samples are aromatic in nature. In addition, the high-quality PPP samples made from **1** behave very differently in the NMR spectrometer compared to the irregular polyphenylenes and phenylene oligomers.

**(iv) Thermal Stability.** Although different combinations of precursors and acid catalyst produce polyphenylenes of different quality, the thermal stabilities of all the polyphenylene samples are quite similar under Ar atmosphere. The thermal stabilities of the six polyphenylene samples made by the catalyzed and uncatalyzed bulk pyrolysis of **1** and **2** were determined by TGA and are summarized in Table 4.

As can be seen in Table 4, the thermal stabilities of the polyphenylene samples made by the uncatalyzed and DCBSA-catalyzed aromatizations of **1** and **2** are essentially identical. They all undergo slow decomposition beginning at approximately 500 °C. These decomposition temperatures are in good agreement with the thermal stabilities of previous "PPP" samples made by other routes in the literature.<sup>6</sup> The high-quality PPP made from **1** and the irregular polyphenylene made from **2** using ZnCl<sub>2</sub> both exhibit significantly lower thermal stabilities. The

lower thermal stability may be the result of the approximately 25 wt % residual ZnCl<sub>2</sub> present in the two samples.

**(v) UV-Visible Spectroscopy.** UV-visible spectroscopy was also used to characterize the polyphenylene samples made from precursors **1** and **2**. Traditionally, the position of the UV-visible absorption maximum ( $\lambda_{\max}$ ) has been used to semiquantitatively gauge the molecular weight and the extent of conjugation of *p*-oligophenyls and "PPP" samples.<sup>6,7,9</sup> The  $\lambda_{\max}$  of *p*-oligophenyls increases asymptotically with increasing chain length.<sup>6</sup>  $\lambda_{\max}$  for an infinitely long PPP chain has been calculated to be 339 nm.<sup>41,42</sup> However,  $\lambda_{\max}$  can only be used to extrapolate the approximate chain length of *p*-oligophenyls and PPP because the relationship between  $\lambda_{\max}$  and chain length loses precision with increasing molecular weight.<sup>6</sup> UV-visible spectroscopy can also be used to detect the presence of structural defects in "PPP" samples and oligophenylenes. For example, polynuclear aromatic units in polyphenylenes made by oxidative polymerization of benzene generally afford excessively high  $\lambda_{\max}$  values of 379–395 nm.<sup>6</sup> Conversely, nonlinear 1,2- and 1,3-linkages in oligophenyls are known to shift the  $\lambda_{\max}$  values of these compounds to lower values compared to those of their completely 1,4-linked analogs.<sup>9,43–45</sup>

Unfortunately, conventional transmission UV-visible spectra of the as-synthesized bulk polyphenylenes made from **1** and **2** could not be obtained due to the opaqueness of the bulk materials. Reflectance UV-visible spectra also could not be obtained because of the unique morphology of the bulk polyphenylene foams made from acid-catalyzed pyrolysis of **1** and **2**.<sup>46</sup> In order to obtain UV-visible spectra, thin films of the precursors and catalysts were baked onto quartz transmission windows and the transmission UV-visible spectra of the resulting pale yellow-brown<sup>47</sup> films were taken. As can be seen in Figure 18, the  $\lambda_{\max}$  values of all of the thin film polyphenylene samples fall short of the value of 339 nm calculated for high molecular weight structurally regular PPP. Two additional observations can be made from a comparison of the six spectra in Figure 18: (1) The polyphenylene film made from the DCBSA-catalyzed aromatization of stereoregular **1** has approximately the same  $\lambda_{\max}$  value (305–310 nm) as the film made

(41) Davydov, A. S. *Zh. Eksp. Teor. Fiz.* **1948**, *18*, 515.

(42) Suzuki, H. *Bull. Chem. Soc. Jpn.* **1960**, *33*, 109.

(43) Ibuki, E.; Ozasa, S.; Fujioka, Y.; Kitamura, H. *Chem. Pharm. Bull.* **1980**, *28* (5), 1468.

(44) Ozasa, S.; Hatada, N.; Fujioka, Y.; Ibuki, E. *Bull. Chem. Soc. Jpn.* **1980**, *53* (9), 2610.

(45) Ibuki, E.; Ozasa, S.; Murai, K. *Bull. Chem. Soc. Jpn.* **1975**, *48* (6), 1868.

(46) Reflectance UV-visible analysis on powders of the bulk polyphenylene samples could not be performed. The resilient "spongy" morphology of some of the samples made them extremely difficult to finely powder and/or press into pellets. In fact, some of the polyphenylene samples could not be ground with a mortar and pestle but rather had to be cut up with a razor for packing into solid-state NMR sample rotors. Attempts to use an amalgamator to grind up the polyphenylene samples with an inert matrix material such as NaCl for spectroscopy were only partially successful. The amalgamated powder samples were not completely homogeneous and were cloudy to the eye when pressed into pellets. Although suitable for FT-IR spectroscopy, the amalgamated samples were unsuitable for UV-visible work.

(47) The bulk polyphenylene samples appear dark brown-black and the thin films appear pale yellow-brown to the naked eye. Although the  $\lambda_{\max}$  of the polyphenylenes is in the UV region of the EM spectrum, the polyphenylene samples appear slightly colored because of the low-intensity absorption tail from the broad main UV band that extends into the visible region (Figure 18). The same yellow-brown color is exhibited by the high-quality PPP thin films made from **1** and *o*-H<sub>3</sub>PO<sub>4</sub> (see ref 48). These high-quality PPP films exhibit a  $\lambda_{\max}$  consistent with theoretic calculations for high molecular weight, structurally regular PPP, but they still appear colored to the naked eye because, again, the broad main UV absorption band tails into the visible region (Figure 19). Thus, the color of the PPP samples made from stereoregular **1** is not indicative of regiochemical defect sites but rather a consequence of the broadness of the main UV absorption band.

(40) Magnetic measurements were performed on a Quantum Design Model MPMS magnetic property measurement system by Dr. S. Josh Jacobs at Caltech.

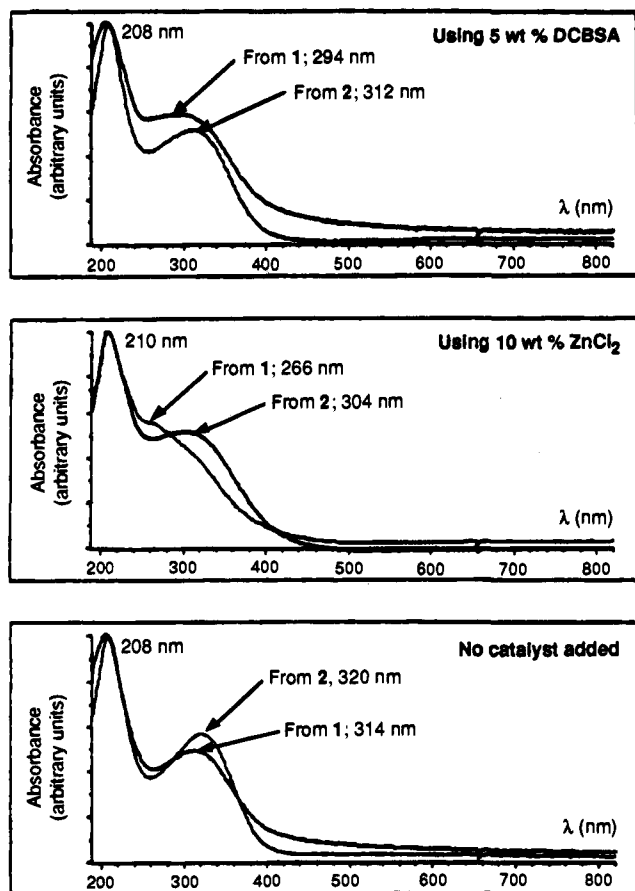


**Figure 18.** UV-visible spectra of polyphenylene films made from the acid-catalyzed and uncatalyzed pyrolyses of thin films of **1** and **2** on quartz wafers.

from the pyrolysis of pristine **1**. This observation is inconsistent with previous IR studies which indicated that the bulk PPP samples made by the acid-catalyzed pyrolysis of **1** have higher molecular weights than the oligomers made from the pristine precursor (see IR Analysis). (2) The bulk polyphenylene samples obtained by the DCBSA- and ZnCl<sub>2</sub>-catalyzed aromatization of **2** have been shown by IR analysis to contain a substantial amount of 1,2-units. However, only the ZnCl<sub>2</sub>-catalyzed thin film made from **2** exhibits the lower  $\lambda_{\max}$  value expected from the presence of these structural defects.

We believe that these anomalous thin film UV-visible results arise from the unsuitability of organic acid catalysts such as DCBSA for thin film conversions of **1** and **2**. As discussed previously in the IR analysis section, polyphenylene samples made by pyrolysis of thin films of the precursors containing organic acids such as DCBSA are probably not representative of the bulk polyphenylenes made using the same catalysts. In thin film pyrolysis where the surface area to mass ratio is extremely high, the organic acids appear to be ineffective because they are too volatile and apparently sublime prior to the onset of conversion. Thus, as in the case of the thin film IR spectra in Figure 13, the UV-visible spectra of the polyphenylene films made from the pristine precursors and those made using organic acid catalysts are essentially the same. ZnCl<sub>2</sub>, on the other hand, remains effective even during thin film pyrolysis because it is nonvolatile and very thermally stable, thereby allowing it to remain in the thin films throughout the thermal conversion process. Consequently, only the polyphenylene thin film made from **2** using ZnCl<sub>2</sub> exhibits the dramatically lower  $\lambda_{\max}$  expected for material containing 1,2-units. The  $\lambda_{\max}$  of the polyphenylene thin film made from **1**

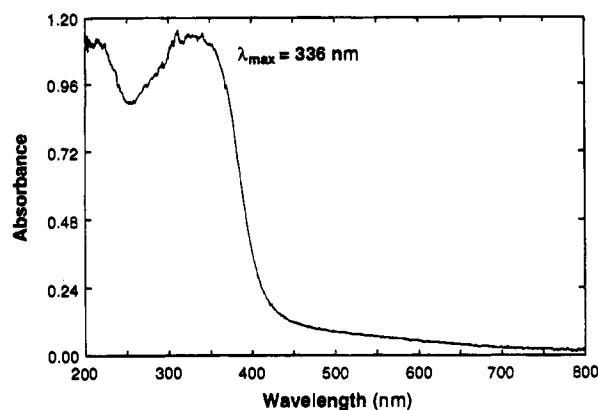


**Figure 19.** UV-visible spectrum of a thin PPP film made from the pyrolysis of **1** using *o*-H<sub>3</sub>PO<sub>4</sub> as the acid catalyst.<sup>48</sup>

using ZnCl<sub>2</sub> is still slightly lower than that expected for high-quality PPP. This discrepancy may be due to the fact that ZnCl<sub>2</sub> is a high-melting solid (mp = 283 °C) and may not be able to easily diffuse through the polyphenylene matrix as it forms to effect uniform catalysis.

As a statement added in proof for these working hypotheses, thin PPP films with  $\lambda_{\max}$  values consistent with high molecular weight, structurally regular PPP were recently synthesized from **1** using a stoichiometric amount of a suitable nonvolatile, thermally stable, Brønsted acid. MacDiarmid et al. recently found that thin PPP films exhibiting  $\lambda_{\max}$  values between 333 and 338 nm can be consistently obtained from **1** by using orthophosphoric acid (*o*-H<sub>3</sub>PO<sub>4</sub>) (86% in H<sub>2</sub>O) as the catalyst in the thin film pyrolysis (Figure 19).<sup>48</sup> *o*-H<sub>3</sub>PO<sub>4</sub> appears to be an ideal solution to the apparent volatility and thermal stability problems exhibited by organic acids such as DCBSA. H<sub>3</sub>PO<sub>4</sub> is a nonvolatile, nonoxidizing liquid acid that dehydrates in stages during heating to form even more thermally stable poly-(metaphosphoric acid). This polymeric acid can then be easily removed from the resulting PPP matrix by hydrolysis back to the water-soluble, monomeric *o*-H<sub>3</sub>PO<sub>4</sub>.<sup>48</sup> Thus, our anomalous thin film IR and UV-visible results stem from a poor choice of acid catalyst for thin film work rather than from the nature of the precursor polymers.

**(vi) Preliminary Doping and DC Conductivity Measurements.** "PPP" samples in the literature are known to form highly conductive charge-transfer complexes when doped with strong electron acceptors (e.g., AsF<sub>5</sub>) or strong electron donors (e.g., alkali metals).<sup>6,7</sup> In fact, DC conductivities of up to 500 S/cm have been measured for AsF<sub>5</sub>-doped pressed powder pellets of "PPP" made by the oxidative cationic polymerization of benzene.<sup>6,7</sup> In order to compare the conductivities of the polyphenylene samples made by our new precursor route, similar AsF<sub>5</sub>-doping experiments were performed and conductivity measurements were taken.

Doping and DC conductivity experiments on polyphenylene samples are usually performed on pressed powder pellets due to the intractable nature of the material.<sup>7</sup> Unfortunately, due to the unique morphology of our acid-catalyzed polyphenylene samples, void-free, pressed powder pellets could not be prepared.<sup>49</sup> Thus, due to morphological and processing limitations, preliminary doping and conductivity experiments had to be performed on two types of polyphenylene samples. The polyphenylenes made from DCBSA- and ZnCl<sub>2</sub>-catalyzed bulk

(48) (a) Gin, D. L.; Avlyanov, J. K.; Min, Y.; MacDiarmid, A. G. *Polym. Prepr. (Am. Chem. Soc., Div. Polym. Chem.)* **1994**, *35* (1), 287. (b) Gin, D. L.; Avlyanov, J. K.; MacDiarmid, A. G. *Synth. Met.* **1994**, *66*, 169.

pyrolysis of **1** and **2** were analyzed as the as-synthesized polyphenylene foams. The polyphenylene oligomers obtained from bulk pyrolysis of the pristine precursors were analyzed as films baked on quartz substrates. It was not possible to prepare all of the samples into a single form for a truly comparative conductivity study because only the acid-catalyzed pyrolysis products form foams whereas the samples made from the pristine precursors form brittle films. Doping and conductivity studies could not all be performed on thin films because the organic acid catalysts employed have been shown to be ineffective in thin film pyrolysis.

The six polyphenylene samples prepared from **1** and **2** were doped by exposing them to approximately 240 Torr of AsF<sub>5</sub> in a vacuum line for 50–60 min at ambient temperature. Only the doped PPP sample made from the DCBSA-catalyzed aromatization of **1** exhibited an appreciably high electrical conductivity of approximately 10<sup>-2</sup>–10<sup>-1</sup> S/cm. The other five doped polyphenylene samples made from **1** or **2** exhibited low bulk conductivities ( $\leq 10^{-6}$  S/cm). The conductivity value measured for the doped PPP foam made by the DCBSA-catalyzed pyrolysis of **1** should be considered a lower limit because of its amorphous, void-filled structure. Significantly higher conductivities may well be possible if the PPP sample is doped for a longer period of time or if it can be processed into an oriented, void-free form.<sup>50</sup>

## Conclusions

The molecular weight and structural regularity of the polyphenylene produced from the thermal conversion of precursor polymers **1** and **2** depend on the stereochemistry of the precursor and the presence of aromatization catalysts. Two competing reactions occur during bulk pyrolysis of these precursors: (1) thermal chain fracturing of the polymer (eq 2) and (2) thermally-induced acid elimination (aromatization) resulting in polyphenylene formation (eq 3). The relative rates of these two processes, which ultimately determine the molecular weight of the final product, depend heavily upon the stereochemistry of the polymer backbone. For the 1,4-linked, stereoregular precursor **1**, the rate of thermal chain fracturing is much greater than the rate of acid elimination during pyrolysis. Consequently, this material only affords low-quality polyphenylene oligomers, despite having a regular stereochemistry that is ideal for facile *cis* pyrolytic acid elimination. On the other hand, the reverse relationship is true for its radically polymerized analog **2**, which has random backbone stereochemistry and 10% regiochemical defects. Although chain degradation still occurs during the pyrolysis of **2**, the relative amount of backbone fracturing is less than that of aromatization. The problems associated with the limited thermal stabilities of both precursor polymers can be overcome by using Brønsted and Lewis acid catalysts during bulk pyrolysis. Strong acids lower the onset temperature of aromatization to a regime well below that at which thermal chain scission can occur by selectively catalyzing the acid elimination reaction. However, characterization of the resulting polyphenylenes made from **1** and **2** indicates that the structural regularity of the polyphenylene produced by the acid-catalyzed aromati-

zation process depends entirely on the regiochemistry of the initial precursor polymer. Only the acid-catalyzed bulk aromatization of the 1,4-linked, stereoregular polymer **1** yields high molecular weight, structurally regular PPP.

The high-quality PPP produced by the acid-catalyzed bulk aromatization of **1** exhibits properties similar to those of previous "PPP" samples in the literature. However, the PPP made from **1** is amorphous whereas "PPP" samples made by other routes are almost always semicrystalline. Because the physical properties of PPP and many other conjugated polymers depend on sample morphology, suitable processing techniques for our PPP have to be developed before its optimum properties can be realized.

## Experimental Section

**General Considerations.** All manipulations were performed in air unless otherwise specified. Reagents, gases, and solvents were used as purchased without further purification unless otherwise specified. Drying of polymers prior to pyrolysis or analysis was performed on a Schlenk line using conventional vacuum line techniques. Air- and/or water-sensitive compounds were stored in a nitrogen-filled Vacuum Atmospheres drybox.

**Materials and Reagents.** Solvents such as THF and hexanes were obtained from the Fisher Scientific Co. or EM Science. 3,4-Dichlorobenzenesulfonic acid (DCBSA) was purchased from the Eastern Chemical Co. Zinc chloride (99.999%) was purchased from the Aldrich Chemical Co. and stored in the drybox. *p*-Toluenesulfonic acid, 2,6-di-*tert*-butyl-4-methylphenol (BHT) (99+%), *p*-terphenyl, and *p*-quaterphenyl were also purchased from the Aldrich Chemical Co. *p*-Sexiphenyl was purchased from TCI America. Argon (UN1006) for tube furnace pyrolysis and TGA experiments was obtained from the Liquid Air Co. Arsenic pentafluoride was purchased from the Ozark-Mahoning Co. NaCl, KBr, and quartz transmission windows (25- × 2-mm discs) were all purchased from the Wilmad Glass Co. Polymer **1** was synthesized according to the procedures outlined in preceding publications and patents.<sup>1,51</sup> Polymer **2** (batch 12871/80) was graciously donated by ICI Chemicals and Polymers Ltd., Runcom, U.K.

**Preparation of Precursor/Catalyst Mixtures for Pyrolysis and TGA Studies.** Typically, a mixture of **1** or **2** containing a specified weight percent of acid catalyst was prepared by dissolving the appropriate amount of precursor polymer in THF, syringing in the appropriate amount of catalyst from a THF stock solution, and coprecipitating the two dispersed components by decanting the mixture into a nonsolvent (e.g., pentane or hexanes). For example, a mixture of **1** containing 10 wt % of ZnCl<sub>2</sub> was prepared by first dissolving the polymer (0.360 g) in THF (6.0 mL). With rapid stirring, 1.20 mL of a 0.033 g/mL stock solution of ZnCl<sub>2</sub> in dry THF was then syringed into the polymer solution. The pale yellow polymer/catalyst solution was then added dropwise to approximately 75 mL of rapidly stirred hexanes containing 0.1% BHT (an antioxidant). The resulting off-white precipitate was isolated by suction filtration, washed with fresh hexanes, and then dried overnight *in vacuo*. The off-white powder was stored in a vial with a PTFE-lined cap and sealed with parafilm to exclude atmospheric moisture. The amount of ZnCl<sub>2</sub> (or other acid catalyst added) in the mixture was confirmed by elemental analysis at Oneida Research Services, Inc., Whitesboro, NY.

**Preparation of Supported Thin Films of Precursor/Catalyst Mixtures for Pyrolysis.** An approximately 15 wt % solution of a pristine precursor polymer or a precursor/catalyst mixture was prepared by dissolving 0.100 g of the powder in 0.6 mL of THF. The viscous polymer solution was then clarified by passing through a small plug of glass microfiber paper (Whatman) in a Pasteur pipette. Four to five drops of the filtered solution were then placed on top of a 25- × 2-mm disc (NaCl, KBr, or quartz) and spin-coated at a speed of (1.6–1.7) × 10<sup>3</sup> rpm for 30 s using a Headway Research spin-coater. Additional

(49) Attempts to form void-free, pressed pellets of powdered DCBSA- and ZnCl<sub>2</sub>-catalyzed polyphenylene samples using a KBr pellet die and 10<sup>5</sup>-lb applied load were unsuccessful. The powders could be compacted under pressure, but the resulting pellets would not hold together. Attempts to form void-free pellets of the DCBSA- and ZnCl<sub>2</sub>-catalyzed polyphenylene samples by pyrolyzing the precursor/catalyst mixtures under pressure in a heated KBr pellet die also failed. The samples were simply extruded out of the die as they aromatized.

(50) Conductivities measured for compacted powder pellets of a polycrystalline material can be up to 100 times lower than that of a completely space-filled, single-crystalline material. See ref 7.

(51) (a) Grubbs, R. H.; Gin, D. L.; Conticello, V. P.; Hampton, P. D.; Wheeler, D. R. U.S. Patent 5 128 418, 1992. (b) Grubbs, R. H.; Gin, D. L.; Conticello, V. P. U.S. Patent 5 122 574, 1992. (c) Grubbs, R. H.; Gin, D. L.; Conticello, V. P. U.S. Patent 5 191 025, 1993.

spinning (30 s) after initial film formation was usually employed to dry the films. Transparent supported films up to 10  $\mu\text{m}$  in thickness were typically obtained by this procedure.

**Preparation of Pressed Powder Pellets for Bulk Pyrolysis and TGA Studies.** The pristine precursor polymer or a precursor polymer/catalyst mixture (100–150 mg) was loaded as a fine powder into a 1.3-cm-i.d. KBr pellet die (Aldrich). The die was placed in a Carver Laboratory Press (Mini "C", 12-ton capacity), and a 10 000-lb load was applied to the die under light vacuum for approximately 0.5–1 min to obtain a firm, free-standing pellet approximately 1 mm in thickness.

**Bulk Pyrolysis Procedure.** Pyrolysis of supported thin films or pressed pellets of the precursor polymers was performed using a Lindberg Model 55437 Moldatherm, three-zone, hinged tube furnace with a 3-in.-i.d.  $\times$  43-in.-long quartz tube insert. The temperatures within the three zones were controlled by a Eurotherm 818P controller/programmer to regulate the middle zone and two Eurotherm 847 digital controllers to regulate the two end zones.

Pressed pellets and supported thin films were placed on flat glass plates inside the quartz tube near the center of the furnace heating area. All samples were dried at 100  $^{\circ}\text{C}$  for 1 h under argon flush prior to the actual pyrolysis run, which was also performed under argon flush. The complete temperature program for pyrolysis of pristine precursors or precursors/organic acid mixtures was as follows:

100  $^{\circ}\text{C}$  (held 1 h)  $\rightarrow$  (2  $^{\circ}\text{C}/\text{min}$ )  $\rightarrow$  300  $^{\circ}\text{C}$  (held 5 h)  $\rightarrow$   
(2  $^{\circ}\text{C}/\text{min}$ )  $\rightarrow$  400  $^{\circ}\text{C}$  (held 0.1 h)  $\rightarrow$  (10  $^{\circ}\text{C}/\text{min}$ )  $\rightarrow$   
50  $^{\circ}\text{C}$  (held 0.5 h)

A slightly different temperature program was employed for precursor polymer mixtures containing  $\text{ZnCl}_2$  because the thermal stabilities of the resulting polyphenylene/ $\text{ZnCl}_2$  composites are slightly lower (see Table 4):

100  $^{\circ}\text{C}$  (held 1 h)  $\rightarrow$  (2  $^{\circ}\text{C}/\text{min}$ )  $\rightarrow$  340  $^{\circ}\text{C}$  (held 5 h)  $\rightarrow$   
(10  $^{\circ}\text{C}/\text{min}$ )  $\rightarrow$  50  $^{\circ}\text{C}$  (held 0.5 h)

Mass losses during the bulk pyrolysis were determined by either comparing the masses of the pellets before and after pyrolysis or by using isothermal TGA, mimicking the tube furnace temperature programs with the Multi-Ramp isothermal software included with the Perkin-Elmer TGA7.

**Thermogravimetric Analysis (TGA).** Thermogravimetric analysis was performed on powders or pieces of pressed pellets using a Perkin-Elmer PC Series TGA7. All TGA samples were dried for 30 min at 100  $^{\circ}\text{C}$  under argon flush in the apparatus prior to the start of each run. Conventional percent weight loss vs temperature profiles were performed under argon flush using platinum sample pans. Typically, samples were heated from a starting temperature of 50 or 100  $^{\circ}\text{C}$  at a ramp rate of 10  $^{\circ}\text{C}/\text{min}$  to a final temperature of 350, 450, or 700  $^{\circ}\text{C}$ .

**Thermogravimetric Analysis–Mass Spectrometry (TGA–MS).** Initial TGA–MS analysis was performed at ICI Chemicals and Polymers, Runcorn, U.K., with a Netzsch STA/QMA system: 409/429–403. Powder and pressed pellet samples were analyzed under a flow of helium (60  $\text{cm}^3/\text{min}$ ) in a platinum crucible. Samples were typically heated from room temperature at 10  $^{\circ}\text{C}/\text{min}$  to a final temperature of either 500 or 600  $^{\circ}\text{C}$ . Additional TGA–MS analyses were performed at the LRSM at the University of Pennsylvania using a TA Instruments 951 thermal analyzer or a Seiko Instruments SSR/5200 TGA/DTA connected to a Fisons Instruments Thermolab mass spectrograph. Powder and pellet samples were analyzed under a flow of argon (Ultrapur, 100  $\text{cm}^3/\text{min}$ ) in a platinum sample pan. Samples were typically heated from room temperature at 10  $^{\circ}\text{C}/\text{min}$  to a final temperature of 400 or 600  $^{\circ}\text{C}$ .

**Infrared (IR) Analysis.** IR spectra of the polyphenylene samples and *p*-oligophenyls were obtained using a Perkin-Elmer 1600 Series FT-IR spectrometer over the 4400–450- $\text{cm}^{-1}$  spectral range with a resolution of 2  $\text{cm}^{-1}$ . Spectra were taken of thin films on NaCl or KBr crystals or as KBr pressed pellet mulls. All spectra were taken under a stream of nitrogen and background corrected by subtracting the spectra of blank substrate material.

**Powder X-ray Diffraction (PXRD).** Wide angle powder X-ray diffraction on the polyphenylene samples was performed on ground-

up pellets with a Scintag/USA PAD V diffractometer using Ni-filtered,  $\text{CuK}\alpha$  radiation. Sample preparation involved adhering the powdered samples onto one side of a 25- $\times$  2-mm glass disc mount with petroleum jelly. The mounted samples were spun and step-scanned for 5 or 10 s every 0.04 $^{\circ}$  over the  $2\theta$  range of 5–50 $^{\circ}$ . The PXRD spectra obtained by this procedure were all background corrected.

**Scanning Electron Microscopy (SEM).** Scanning electron microscope images of the bulk PPP samples were obtained using a CamScan scanning electron microscope. The samples were generally cut in two by a razor blade to expose the interior cross section. The cleaved samples were then mounted onto stainless steel stubs with graphite paint and then gold-coated prior to SEM imaging.

**$^{13}\text{C}$  CPMAS Solid-State NMR Analysis.**  $^{13}\text{C}$  CPMAS solid-state NMR spectra were obtained on a Bruker MSL-200 (200.13-MHz  $^1\text{H}$ , 50.32-MHz  $^{13}\text{C}$ ) spectrometer. NMR samples were generally prepared by powdering the samples with an agate mortar and pestle and packing them into 0.5-cm-o.d. zirconium oxide rotors mated with Kel-F caps. If insufficient sample was available to completely pack a rotor, the sample was diluted with alumina (Fluka). Rough shimming of the spectrometer field prior to the runs was performed on a static sample of  $\text{H}_2\text{O}$ . The Hartmann–Hahn condition was tuned by optimizing the shape of the free induction decay trace of a sample of adamantane, followed by further shimming of the field on the same sample.  $^{13}\text{C}$  CPMAS NMR spectra of the polyphenylenes and *p*-oligophenyls were obtained on samples spun at 3.4–3.5 kHz at a temperature of 300 K. Common pulse parameters employed for all samples were a  $^1\text{H}$  90 $^{\circ}$  pulse of 6  $\mu\text{s}$  and a dwell time of 4  $\mu\text{s}$ . Typically, 800–7000 scans were taken for each spectrum. Spectra of semicrystalline polyphenylene and *p*-oligophenyl samples were taken using a contact time of 10 ms and an acquisition time of 100 ms, whereas optimum spectra of the amorphous polyphenylene samples were obtained using a contact time of 1 ms and an acquisition time of 200 ms. A recycle delay time of 5 s was more than adequate for all the polyphenylene samples, but longer recycle delays on the order of 100–400 s were required for *p*-quaterphenyl and *p*-sexiphenyl because of their much larger  $^1\text{H}$   $T_1$  values. Generally a line broadening factor of 50 Hz was applied to all FID's prior to Fourier transformation to improve the signal-to-noise level in the displayed spectra.

$^1\text{H}$   $T_1$  values were calculated for some of the polyphenylene samples using the inversion–recovery method.<sup>34,52,53</sup> For each sample, several spectra were taken with different variable delay times ( $\tau$ ) but with the same number of scans using the following pulse sequence:

180 $^{\circ}$ – $\tau$ –(cross-polarization pulse sequence)

For the series of spectra, the absolute intensity of the peak at 128 ppm as a function of  $\tau$  was curve-fitted to extrapolate a value for  $^1\text{H}$   $T_1$ .

**UV–Visible Spectroscopy.** UV–visible spectra of thin polyphenylene films were obtained with a Hewlett-Packard Model 8452A diode array spectrophotometer. Samples were prepared by spin-coating 6–8 drops of filtered precursor or precursor/catalyst solutions (20 mg in 0.5 mL of THF) onto 25- $\times$  2-mm quartz discs using a spinning speed of 1000 rpm and a spinning time of 30 s. The supported thin films were then pyrolyzed according to the procedure outlined in the section entitled Bulk Pyrolysis Procedure. UV–visible spectra of the resulting transparent, light yellow-brown films were taken in air over the 190–820-nm spectral range using a blank quartz disc as the background correction.

**AsF<sub>5</sub> Doping.** AsF<sub>5</sub> doping of the polyphenylene samples was performed according to the procedure of Swager.<sup>54</sup> Due to the toxicity of the dopant, a dedicated single-manifold vacuum line in a high-speed fumehood containing a charcoal filter was used. All valves on the line were constructed of PTFE, and all connections for attaching glassware were Viton O-ring seals. The O-rings were coated with Halocarbon grease (Halocarbon Products Corp.) to provide extra resistance to strong oxidizers. Pressure in the line was measured using

(52) Kowalewski, J.; Levy, G. C.; Johnson, L. F.; Palmer, L. J. *Magn. Reson.* 1977, 26, 533.

(53) Sullivan, M. J.; Maciel, G. E. *Anal. Chem.* 1982, 54, 1615.

(54) Swager, T. M. Ph.D. Thesis, California Institute of Technology, 1988.

an electronic gauge system specially designed for use with corrosive gases: a MKS Instruments AA01000A pressure transducer and a PDRC-1B readout/power supply unit with a precision of 0.1 Torr. Both the pressure transducer and the AsF<sub>5</sub> tank were connected to the line via separate metal-to-glass seals. Samples for exposure to AsF<sub>5</sub> were loaded in thick-walled glass, wide-bore doping chambers containing O-ring seals and a PTFE valve to control gas flow.

A typical doping experiment first involved degassing the entire line under dynamic vacuum up to the AsF<sub>5</sub> tank while heating the glass sections. Under static vacuum, 300 Torr of AsF<sub>5</sub> was slowly admitted into the line. The dopant was then condensed into a cold finger immersed in liquid nitrogen and degassed for 15 min under dynamic vacuum. With the AsF<sub>5</sub> still frozen in the cold finger, the doping chambers containing the polyphenylene samples were attached to the line and thoroughly degassed under dynamic vacuum for approximately 30 min. The AsF<sub>5</sub> in the cold finger was allowed to slowly warm up to room temperature and fill the manifold and the doping chambers with a total pressure of 238 Torr of dopant. After approximately 50 min of exposure, the excess AsF<sub>5</sub> was condensed back into the cold finger. The cold finger was then detached from the line, and the excess AsF<sub>5</sub> was quenched with acetone while still in the solid or liquid state. The doped samples were degassed for 8–10 h under dynamic vacuum to remove any traces of excess dopant before transferring them to the drybox for DC conductivity measurements.

**DC Conductivity Measurements.** All DC conductivity measurements on doped polyphenylene samples were performed in the drybox using a four-in-line probe system<sup>7</sup> consisting of a Signatone four-in-line probe head (probe spacing of 0.15 cm), a Signatone combination sample support/probe arm, two Kiethley Model 197 autoranging digital multimeters, and a Power Designs Model 605 precision power source. DC conductivity values ( $\sigma$ ) were obtained by placing the four probes on the surface of the doped pellets or films, applying a potential via the power source, and measuring the resulting current ( $i$ ) between the two outer probes and the voltage drop ( $v$ ) across the two inner probes. The bulk conductivity is calculated according to eq 5:<sup>7</sup>

$$\sigma = \frac{1}{2\pi S} \frac{i}{v} \quad (5)$$

This equation applies for samples thicker than the probe spacing ( $S$ ).<sup>7</sup> Sample thicknesses were measured with a Fowler Digitrix II electronic caliper for the pellets or a Dektak 3030 profilometer for the supported thin films. Reported DC conductivity values were an average of a series of  $i$  and  $v$  measurements taken over a range of applied voltages (0.1–1.5 V) from the power supply. Initial measurements were performed on a commercial Si wafer ( $\sigma = 100$ – $200$  S/cm) to confirm

the accuracy of the detection circuit prior to actual measurements on the doped samples. Generally, conductivity values below  $10^{-6}$  S/cm could not be measured accurately with the detection circuit described above.

**Differential Scanning Calorimetry (DSC).** DSC profiles included in the Supplementary Material were obtained on pressed powder pellets of the precursors using a TA Instruments DSC 2920 differential scanning calorimeter. All samples were analyzed under nitrogen flush using a temperature ramp rate of 5 °C/min.

**Acknowledgment.** We are grateful for financial support from the Air Force Office of Scientific Research (Grant AFOSR-88-0094). We would like to thank Dr. D. G. H. Ballard, Dr. D. M. Haddleton, Dr. A. V. G. Muir, Mr. A. Nevin, Mr. E. A. Roberts, and Dr. G. Wilkinson at ICI Chemicals and Polymers Ltd., Runcorn, U.K., for providing us with starting materials, samples of polymer **2**, and TGA–MS analyses. We would also like to thank Dr. A. R. McGhie and Professor A. G. MacDiarmid at the University of Pennsylvania for providing us with additional DSC and TGA–MS data. We also thank Dr. D. R. Wilson at Advanced Polymer Technologies, Inc., for a preprint of his work and for helpful discussions. D.L.G. gratefully acknowledges the Natural Sciences and Engineering Research Council of Canada for a 1967 Science and Engineering Scholarship while at Caltech.

**Supplementary Material Available:** Figures containing additional MS profiles of **1** containing 5 wt % DCBSA, 10 wt % ZnCl<sub>2</sub>, and no acid catalysts, showing the evolution of other significant compounds detected during TGA; a plot of  $T_{\text{onset}}$  vs wt % ZnCl<sub>2</sub> added for the bulk pyrolysis of **1**; DSC profiles of pristine **1** and mixtures of **1** containing 5 wt % DCBSA and 10 wt % ZnCl<sub>2</sub>; TGA and MS profiles showing the evolution of acetic acid, benzene, and phenol for **2** containing 5 wt % DCBSA and 10 wt % ZnCl<sub>2</sub>; and full window FT-IR spectra (4400–450 cm<sup>-1</sup>), PXRD profiles, and TGA profiles (under Ar flush) of the bulk polyphenylene samples made from **1** and **2** with and without the acid catalyst (30 pages). This material is contained in many libraries on microfiche, immediately follows this article in the microfilm version of the journal, and can be ordered from the ACS; see any current masthead page for ordering information.